Long-range two-particle correlations of strange hadrons with charged particles in pPb and PbPb collisions at LHC energies

CMS Collaboration [*]

CERN, Switzerland

ABSTRACT

Measurements of two-particle angular correlations between an identified strange hadron (K_S^0 or $\Lambda/\overline{\Lambda}$) and a charged particle, emitted in pPb collisions, are presented over a wide range in pseudorapidity and full azimuth. The data, corresponding to an integrated luminosity of approximately 35 nb^{-1}, were collected at a nucleon–nucleon center-of-mass energy ($\sqrt{s_{NN}}$) of 5.02 TeV with the CMS detector at the LHC. The results are compared to semi-peripheral PbPb collision data at $\sqrt{s_{NN}} = 2.76$ TeV, covering similar charged-particle multiplicities in the events. The observed azimuthal correlations at large relative pseudorapidity are used to extract the second-order (v_2) and third-order (v_3) anisotropy harmonics of K_S^0 and $\Lambda/\overline{\Lambda}$ particles. These quantities are studied as a function of the charged-particle multiplicity in the event and the transverse momentum of the particles. For high-multiplicity pPb events, a clear particle species dependence of v_2 and v_3 is observed. For $p_T < 2$ GeV, the v_2 and v_3 values of K_S^0 particles are larger than those of $\Lambda/\overline{\Lambda}$ particles at the same p_T. This splitting effect between two particle species is found to be stronger in pPb than in PbPb collisions in the same multiplicity range. When divided by the number of constituent quarks and compared at the same transverse kinetic energy per quark, both v_2 and v_3 for K_S^0 particles are observed to be consistent with those for $\Lambda/\overline{\Lambda}$ particles at the 10% level in pPb collisions. This consistency extends over a wide range of particle transverse kinetic energy and event multiplicities.

1. Introduction

Studies of multiparticle correlations provide an important insight into the underlying mechanism of particle production in high-energy collisions of protons and nuclei. A key feature of such correlations in ultrarelativistic nucleus–nucleus (AA) collisions is the observation of a pronounced structure on the near side (relative azimuthal angle $|\Delta\phi| \approx 0$) that extends over a large range in relative pseudorapidity ($|\Delta\eta|$ up to 4 units or more). This feature, known as the "ridge", has been found over a wide range of AA energies and system sizes at both the Relativistic Heavy Ion Collider (RHIC) [1–5] and the Large Hadron Collider (LHC) [6–10] and is interpreted as arising primarily from the collective hydrodynamic flow of a strongly interacting, expanding medium [11,12].

Similar long-range correlations have also been discovered in proton–proton (pp) [13], proton–lead (pPb) [14–16], and deuteron–gold (dAu) [17] collisions with high final-state particle multiplicity. As the collision volume size is reduced, it is possible that the

system will not be able to equilibrate and the hydrodynamic description will break down. As such, there has been no consensus on the origin of the particle correlation structure in these smaller systems. A variety of theoretical models have been proposed to interpret this phenomenon in pp [18], pPb, and dAu collisions. Besides hydrodynamic effects in a high-density system [19,20], an alternate model including gluon saturation in the incoming nucleons has also been shown to describe these data [21,22].

In hydrodynamical descriptions, the collective flow manifests itself as an azimuthal anisotropy in the distribution of final-state particles. An additional key consequence of these models is that the measured anisotropies will depend on the mass of the particle [23–25]. More specifically, for particles with transverse momentum below about 2 GeV, the anisotropy will be larger for lighter particles. The presence of this mass ordering is well established in AA collisions at RHIC and LHC energies [26–30]. This phenomenon has recently also been observed in pPb [31] and dAu [17] collisions, consistent with expectations from hydrodynamic models [32,33]. The analysis presented in this paper aims to further explore this effect by extracting anisotropies of identified strange

mesons (K_S^0) and baryons (Λ and $\overline{\Lambda}$) in pPb and in PbPb collisions that produce similar final-state particle multiplicity.

The azimuthal correlations of emitted particle pairs are typically characterized by their Fourier components, $\frac{dN^{pair}}{d\Delta\phi} \propto 1 + \sum_n 2V_{n\Delta} \cos(n\Delta\phi)$, where $V_{n\Delta}$ are the two-particle Fourier coefficients and $v_n = \sqrt{V_{n\Delta}}$ denote the single-particle anisotropy harmonics [34]. In particular, the second and third Fourier components are known as elliptic (v_2) and triangular (v_3) flow, respectively [12]. In hydrodynamical models, v_2 and v_3 are directly related to the response of the medium to the initial collision geometry and its fluctuations [35–37]. As such, these Fourier components can provide insight into the fundamental transport properties of the medium.

In AA collisions at RHIC, a scaling of v_2 as a function of p_T with the number of constituent quarks (n_q) has been observed in the range $2 < p_T < 6$ GeV [38]. Specifically, the values of v_2/n_q are found to be very similar for all mesons ($n_q = 2$) and baryons ($n_q = 3$) when compared at the same value of p_T/n_q. This empirical scaling may indicate that final-state hadrons are formed through recombination of quarks in this p_T regime [39–41], possibly providing evidence of deconfinement of quarks and gluons in these systems. At lower p_T ($p_T < 2$ GeV), a similar scaling behavior is observed, although, according to perfect fluid hydrodynamics, v_2/n_q values must be compared at the same transverse kinetic energy per constituent quark (KE_T/n_q, where $KE_T = \sqrt{m^2 + p_T^2} - m$) to account for the mass difference of hadrons [42,43].

This paper presents an analysis of two-particle correlations with identified strange hadrons, K_S^0 and $\Lambda/\overline{\Lambda}$, in pPb collisions at a center-of-mass energy per nucleon pair ($\sqrt{s_{NN}}$) of 5.02 TeV. With the implementation of a dedicated high-multiplicity trigger, the 2013 pPb data sample gives access to multiplicities comparable to those in semi-peripheral PbPb collisions. Two-particle correlation functions are constructed by associating a K_S^0 or $\Lambda/\overline{\Lambda}$ particle with a charged particle (pairs of K_S^0 or $\Lambda/\overline{\Lambda}$ particles are not studied due to their limited statistical precision). In the context of hydrodynamic models, Fourier coefficients of dihadron correlations can be factorized into products of single-particle azimuthal anisotropies. Assuming that this relationship holds, v_2 and v_3 are extracted from long-range two-particle correlations as a function of strange hadron p_T and event multiplicity. To examine the validity of constituent quark number scaling, v_2/n_q and v_3/n_q are obtained as a function of KE_T/n_q for both K_S^0 and $\Lambda/\overline{\Lambda}$ particles. A direct comparison of the pPb and PbPb results over a broad range of similar multiplicities is presented.

2. The CMS experiment and data sample

A description of the CMS detector in the LHC at CERN can be found in Ref. [44]. The main detector component used in this paper is the tracker, located in a superconducting solenoid of 6 m internal diameter, providing a magnetic field of 3.8 T. The tracker consists of 1440 silicon pixel and 15 148 silicon strip detector modules, covering the pseudorapidity range $|\eta| < 2.5$. For hadrons with $p_T \approx 1$ GeV and $|\eta| \approx 0$, the impact parameter (distance of closest approach from the primary collision vertex) resolution is approximately 100 μm and the p_T resolution is 0.8%.

Also located inside the solenoid are the electromagnetic calorimeter (ECAL) and the hadron calorimeter (HCAL). The ECAL consists of 75 848 lead tungstate crystals, arranged in a quasi-projective geometry and distributed in a barrel region ($|\eta| < 1.48$) and two endcaps that extend to $|\eta| = 3.0$. The HCAL barrel and endcaps are sampling calorimeters composed of brass and scintillator plates, covering $|\eta| < 3.0$. Iron/quartz-fiber forward calorimeters (HF) are placed on each side of the interaction region, covering

$2.9 < |\eta| < 5.2$. The detailed Monte Carlo (MC) simulation of the CMS detector response is based on GEANT4 [45].

The data sample used in this analysis was collected with the CMS detector during the LHC pPb run in 2013. The total integrated luminosity of the data set is about 35 nb^{-1} [46]. The beam energies are 4 TeV for protons and 1.58 TeV per nucleon for lead nuclei, resulting in a center-of-mass energy per nucleon pair of 5.02 TeV. The direction of the proton beam was initially set up to be clockwise (20 nb^{-1}), and was later reversed (15 nb^{-1}). As a result of the energy difference between the colliding beams, the nucleon–nucleon center-of-mass in the pPb collisions is not at rest with respect to the laboratory frame. Massless particles emitted at $\eta_{cm} = 0$ in the nucleon–nucleon center-of-mass frame will be detected at $\eta = -0.465$ (clockwise proton beam) or 0.465 (counterclockwise proton beam) in the laboratory frame. A sample of peripheral PbPb data at $\sqrt{s_{NN}} = 2.76$ TeV corresponding to an integrated luminosity of about 2.3 μb^{-1}, collected during the 2011 LHC heavy-ion run, is also analyzed for comparison with pPb data at similar charged-particle multiplicity ranges.

3. Online triggering and offline track reconstruction and selection

The online triggering and the offline reconstruction and selection follow the same procedure as described in Ref. [47]. Minimum bias pPb events are triggered by requiring at least one track with $p_T > 0.4$ GeV to be found in the pixel tracker for a pPb bunch crossing. Because of hardware limits on the data acquisition rate, only a small fraction ($\sim 10^{-3}$) of all minimum bias triggered events are recorded. In order to collect a large sample of high-multiplicity pPb collisions, a dedicated high-multiplicity trigger is also implemented using the CMS Level 1 (L1) and high-level trigger (HLT) systems. At L1, two event streams were triggered by requiring the total transverse energy summed over ECAL and HCAL to be greater than 20 or 40 GeV. Charged tracks are then reconstructed online at the HLT using the three layers of pixel detectors, and requiring a track origin within a cylindrical region of 30 cm length along the beam and 0.2 cm radius perpendicular to the beam. For each event, the number of pixel tracks (N_{trk}^{online}) with $|\eta| < 2.4$ and $p_T > 0.4$ GeV is counted separately for each vertex. Only tracks with a distance of closest approach of 0.4 cm or less to one of the vertices are included. The online selection requires N_{trk}^{online} for the vertex with the most tracks to exceed a specific value. Data are taken with thresholds of $N_{trk}^{online} > 100, 130$ (from events with L1 threshold of 20 GeV), and 160, 190 (from events with L1 threshold of 40 GeV). While all events with $N_{trk}^{online} > 190$ are accepted, only a fraction of the events from the other thresholds are kept. This fraction is dependent on the instantaneous luminosity. Data from both the minimum bias trigger and high-multiplicity trigger are retained for offline analysis.

In the offline analysis, hadronic collisions are selected by the presence of at least one tower with energy above 3 GeV in each of the two HF calorimeters. Events are also required to contain at least one reconstructed primary vertex within 15 cm of the nominal interaction point along the beam axis and within 0.15 cm transverse to the beam trajectory. At least two reconstructed tracks are required to be associated with the primary vertex, a condition that is important only for minimum bias events. Beam related background is suppressed by rejecting events for which less than 25% of all reconstructed tracks pass the *high-purity* selection (as defined in Ref. [48]). The pPb instantaneous luminosity provided by the LHC in the 2013 run resulted in a 3% probability of having at least one additional interaction present in the same bunch crossing (pile-up events). The procedure used for rejecting pile-up events is described in Ref. [47] and is based on the number of tracks as-

sociated with each reconstructed vertex and the distance between different vertices. A purity of 99.8% for single pPb collision events is achieved for the highest multiplicity pPb interactions studied in this paper. With the selection criteria above, 97–98% of the events are found to be selected among those pPb interactions simulated with the EPOS LHC [49] and HIJING 2.1 [50] event generators that have at least one particle from the pPb interaction with energy $E > 3$ GeV in each of the η ranges $-5 < \eta < -3$ and $3 < \eta < 5$.

In this analysis, *high-purity* tracks are used to select primary tracks (tracks originating from the pPb interaction). Additional requirements are applied to enhance the purity of primary tracks. The significance of the separation along the beam axis (z) between the track and the best vertex, $d_z/\sigma(d_z)$, and the significance of the impact parameter relative to the best vertex transverse to the beam, $d_T/\sigma(d_T)$, must be less than 3, and the relative p_T uncertainty, $\sigma(p_T)/p_T$, must be less than 10%. To ensure high tracking efficiency and to reduce the rate of misreconstructed tracks, primary tracks with $|\eta| < 2.4$ and $p_T > 0.3$ GeV are used in the analysis (a p_T cutoff of 0.4 GeV is used in the multiplicity determination to match the HLT requirement). Based on simulation studies using GEANT4 to propagate particles from the HIJING event generator, the combined geometrical acceptance and efficiency for primary track reconstruction exceeds 60% for $p_T \approx 0.3$ GeV and $|\eta| < 2.4$. The efficiency is greater than 90% in the $|\eta| < 1$ region for $p_T > 0.6$ GeV. For the event multiplicity range studied in this paper, no dependence of the tracking efficiency on multiplicity is found and the rate of misreconstructed tracks is 1–2%.

The entire pPb data set is divided into classes based on the reconstructed track multiplicity, $N_{\mathrm{trk}}^{\mathrm{offline}}$, where primary tracks with $|\eta| < 2.4$ and $p_T > 0.4$ GeV are counted. Details of the multiplicity classification in this analysis, including the fraction of the full multiplicity distribution and the average number of primary tracks before and after correcting for detector effects in each multiplicity range, are provided in Ref. [47].

A subset of semi-peripheral PbPb data collected during the 2011 LHC heavy-ion run with a minimum bias trigger are also reanalyzed in order to directly compare pPb and PbPb systems at the same collision multiplicity. The reanalyzed events were in the range of 50–100% centrality, where centrality is defined as the fraction of the total inelastic cross section, with 0% denoting the most central collisions. This sample was reprocessed using the same event selection and track reconstruction algorithm as for the present pPb analysis. A description of the 2011 PbPb data can be found in Refs. [47,51].

4. Reconstruction of K_S^0 and $\Lambda/\overline{\Lambda}$ candidates

The reconstruction technique for K_S^0 and $\Lambda/\overline{\Lambda}$ candidates (generally referred to as V^0s) at CMS was first described in Ref. [52]. To increase the efficiency for tracks with low momentum and large impact parameters, both characteristic of the K_S^0 and $\Lambda/\overline{\Lambda}$ decay products, the standard *loose* selection of tracks (as defined in Ref. [48]) is used in reconstructing the K_S^0 and $\Lambda/\overline{\Lambda}$ candidates. Oppositely charged tracks with at least 4 hits and both transverse and longitudinal impact parameter significances greater than 1 (with respect to the primary vertex) are first selected to form a secondary vertex. The distance of closest approach of the pair of tracks is required to be less than 0.5 cm. The fitted vertex in x, y, z of each pair of tracks is required to have a χ^2 value normalized by the number of degrees of freedom less than 7. The pair of tracks is assumed to be $\pi^+\pi^-$ in K_S^0 reconstruction, while the assumption of $\pi^-\mathrm{p}$ ($\pi^+\overline{\mathrm{p}}$) is used in Λ ($\overline{\Lambda}$) reconstruction. For $\Lambda/\overline{\Lambda}$, the lower-momentum track is assumed to be the pion.

Due to the long lifetime of K_S^0 and $\Lambda/\overline{\Lambda}$ particles, a requirement on the significance of the V^0 decay length, which is the

three-dimensional distance between the primary and V^0 vertices divided by its uncertainty, to be greater than 5 is applied to reduce background contributions. To remove K_S^0 candidates misidentified as $\Lambda/\overline{\Lambda}$ particles and vice versa, the $\Lambda/\overline{\Lambda}$ (K_S^0) candidates must have a corresponding $\pi^+\pi^-$ ($\mathrm{p}\pi^-$) mass more than 20 (10) MeV away from the PDG value of the K_S^0 (Λ) mass [53]. The angle θ^{point} between the V^0 momentum vector and the vector connecting the primary and V^0 vertices is required to satisfy $\cos\theta^{\mathrm{point}} > 0.999$. This reduces the effect of nuclear interactions, random combinations of tracks, and $\Lambda/\overline{\Lambda}$ particles originating from weak decays of Ξ and Ω^- particles. From MC simulations using GEANT4 and the HIJING event generator, it is found that the contribution of $\Lambda/\overline{\Lambda}$ particles from weak decays is less than 3% after this requirement. The K_S^0 ($\Lambda/\overline{\Lambda}$) reconstruction efficiency is about 6% (1%) for $p_T \approx 1$ GeV and 20% (10%) for $p_T > 3$ GeV within $|\eta| < 2.4$. This efficiency includes the effects of acceptance and the branching ratio for V^0 particle decays into neutral particles. The relatively low reconstruction efficiency of the V^0 candidates is primarily due to the decay length cut and the low efficiency for reconstructing daughter tracks with $p_T < 0.3$ GeV or large impact parameters.

Examples of invariant mass distributions of reconstructed K_S^0 and $\Lambda/\overline{\Lambda}$ candidates are shown in Fig. 1 for pPb data, with V^0 p_T in the range of 1–3 GeV and event multiplicity in the range $220 \le N_{\mathrm{trk}}^{\mathrm{offline}} < 260$. Since the results for Λ and $\overline{\Lambda}$ are found to be consistent, they have been combined in this analysis. The V^0 peaks can be clearly identified with little background. The true V^0 signal peak is well described by a double Gaussian function (with a common mean), while the background is modeled by a 4th-order polynomial function fit over the entire mass range shown in Fig. 1. The mass window of $\pm 2\sigma$ wide around the center of the peak is defined as the "peak region", where σ represents the root mean square of the two standard deviations of the double Gaussian functions weighted by the yields (with typical value of σ indicated in Fig. 1). To estimate the contribution of background candidates in the peak region to the correlation measurement, a "sideband region" is chosen that includes V^0 candidates from outside the $\pm 3\sigma$ mass range around the V^0 mass to the limit of the mass distributions shown in Fig. 1.

5. Analysis of two-particle correlations

The construction of the two-particle correlation function follows the same procedure established in Refs. [6,7,14,47]. However, in this paper, reconstructed V^0 candidates from either the peak or sideband region are taken as "trigger" particles within a given p_T^{trig} range, instead of charged tracks as used in previous publications. The number of trigger V^0 candidates in the event is denoted by N_{trig}. Particle pairs are formed by associating each trigger particle with the remaining charged primary tracks in a specified p_T^{assoc} interval (which can be either the same as or different from the p_T^{trig} range). The two-dimensional (2D) correlation function is defined in the same way as in previous analyses as

$$\frac{1}{N_{\mathrm{trig}}} \frac{\mathrm{d}^2 N^{\mathrm{pair}}}{\mathrm{d}\Delta\eta\,\mathrm{d}\Delta\phi} = B(0,0) \times \frac{S(\Delta\eta,\Delta\phi)}{B(\Delta\eta,\Delta\phi)}, \tag{1}$$

where $\Delta\eta$ and $\Delta\phi$ are the differences in η and ϕ of the pair. The same-event pair distribution, $S(\Delta\eta,\Delta\phi)$, represents the yield of particle pairs normalized by N_{trig} from the same event,

$$S(\Delta\eta,\Delta\phi) = \frac{1}{N_{\mathrm{trig}}} \frac{\mathrm{d}^2 N^{\mathrm{same}}}{\mathrm{d}\Delta\eta\,\mathrm{d}\Delta\phi}. \tag{2}$$
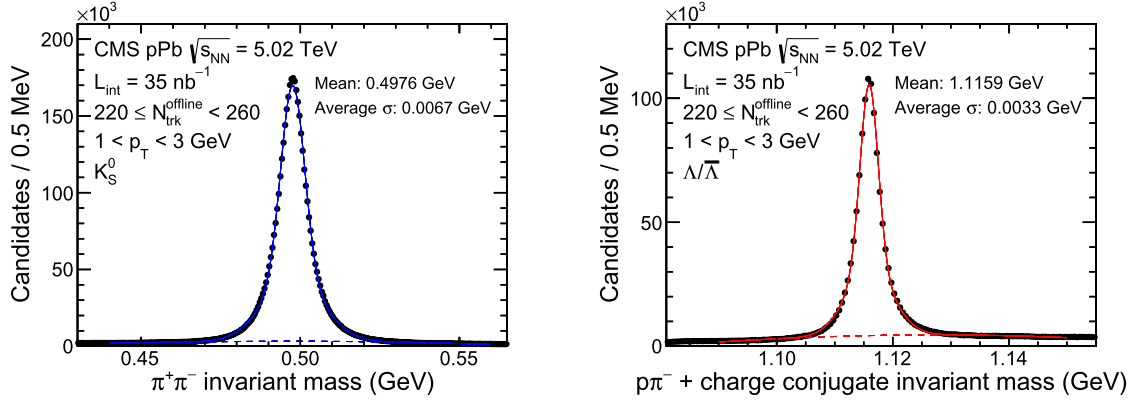
Fig. 1. Invariant mass distribution of K_S^0 (left) and $\Lambda/\overline{\Lambda}$ (right) candidates in the p_T range of 1–3 GeV for $220 \leq N_{trk}^{offline} < 260$ in pPb collisions at $\sqrt{s_{NN}} = 5.02$ TeV. The solid line shows the fit function of a double Gaussian plus a 4th-order polynomial (dashed line).

The mixed-event pair distribution,

$$B(\Delta\eta, \Delta\phi) = \frac{1}{N_{trig}} \frac{d^2 N^{mix}}{d\Delta\eta \, d\Delta\phi}, \tag{3}$$

is constructed by pairing the trigger V^0 candidates in each event with the associated charged primary tracks from 20 different randomly selected events in the same 2 cm wide range of vertex position in the z direction and from the same track multiplicity class. Here, N^{mix} denotes the number of pairs taken from the mixed events. The ratio $B(0,0)/B(\Delta\eta, \Delta\phi)$ mainly accounts for the pair acceptance effects, with $B(0,0)$ representing the mixed-event associated yield for both particles of the pair going in approximately the same direction and thus having maximum pair acceptance (with a bin width of 0.3 in $\Delta\eta$ and $\pi/16$ in $\Delta\phi$). Thus, the quantity in Eq. (1) is effectively the per-trigger-particle associated yield. A pair is removed if the associated particle belongs to a daughter track of any trigger V^0 candidate (this contribution is negligible since associated particles are mostly primary tracks).

The same-event and mixed-event pair distributions are first calculated for each event, and then averaged over all the events within the track multiplicity class. The range of $0 < |\Delta\eta| < 4.8$ and $0 < |\Delta\phi| < \pi$ is used to fill one quadrant of the $(\Delta\eta, \Delta\phi)$ histograms, with the other three quadrants filled (for illustration purposes) by reflection to cover a $(\Delta\eta, \Delta\phi)$ range of $-4.8 < \Delta\eta < 4.8$ and $-\pi/2 < \Delta\phi < 3\pi/2$ for the 2D correlation functions, as will be shown later in Fig. 2. In performing the correlation analyses, each reconstructed primary track and V^0 candidate is weighted by a correction factor, following the procedure described in Refs. [6,7,14,47]. This correction is also applied in calculating N_{trig}. This factor accounts for detector effects including the reconstruction efficiency, the detector acceptance, and the fraction of misreconstructed tracks. This correction factor is found to have a negligible effect on the azimuthal anisotropy harmonics.

5.1. Extraction of v_n harmonics

Motivated by hydrodynamic models of long-range correlations in pPb collisions, azimuthal anisotropy harmonics of K_S^0 and $\Lambda/\overline{\Lambda}$ particles are extracted via a Fourier decomposition of $\Delta\phi$ correlation functions averaged over $|\Delta\eta| > 2$ (to remove short-range correlations such as jet fragmentation),

$$\frac{1}{N_{trig}} \frac{dN^{pair}}{d\Delta\phi} = \frac{N_{assoc}}{2\pi} \left[1 + \sum_n 2 V_{n\Delta} \cos(n\Delta\phi) \right], \tag{4}$$

as was done in Refs. [6,7,14,47]. Here, $V_{n\Delta}$ are the Fourier coefficients and N_{assoc} represents the total number of pairs per trigger

V^0 particle for a given $(p_T^{trig}, p_T^{assoc})$ bin. The first three Fourier terms are included in the fits to the correlation functions. Including additional terms has a negligible effect on the results of the Fourier fit.

If the observed two-particle azimuthal correlations arise purely as the result of convoluting anisotropic distributions of single particles, then the $V_{n\Delta}$ coefficients can be factorized into the product of single-particle anisotropies [47],

$$V_{n\Delta}(p_T^{trig}, p_T^{assoc}) = v_n(p_T^{trig}) \times v_n(p_T^{assoc}). \tag{5}$$

Following this assumption, the elliptic (v_2) and triangular (v_3) anisotropy harmonics of V^0 particles can be extracted as a function of p_T from the fitted Fourier coefficients,

$$v_n(p_T^{V^0}) = \frac{V_{n\Delta}(p_T^{V^0}, p_T^{ref})}{\sqrt{V_{n\Delta}(p_T^{ref}, p_T^{ref})}}, \quad n = 2, 3. \tag{6}$$

Here, a fixed p_T^{ref} range for the "reference" charged primary particles is chosen to be $0.3 < p_T < 3.0$ GeV (the lowest p_T region accessible by CMS and the same as was used in Ref. [47]), to minimize correlations from back-to-back jets at higher p_T.

The v_n values are first extracted for V^0 candidates from the peak region (which contains small contributions from background V^0s) and sideband region, denoted as v_n^{obs} and v_n^{bkg}, respectively. The v_n signal of true V^0 particles is denoted by v_n^{sig} and is obtained by

$$v_n^{sig} = \frac{v_n^{obs} - (1 - f^{sig}) \times v_n^{bkg}}{f^{sig}}, \quad n = 2, 3, \tag{7}$$

assuming v_n^{sig} and v_n^{bkg} are independent from each other. Here, f^{sig} represents the signal yield fraction in the peak region determined by the fits to the mass distribution shown in Fig. 1. This fraction exceeds 80% for $\Lambda/\overline{\Lambda}$ candidates at $p_T > 1$ GeV and is above 95% for K_S^0 candidates over the entire p_T range.

5.2. Systematic uncertainties

Table 1 summarizes different sources of systematic uncertainties in v_n^{sig} (identical for K_S^0 and $\Lambda/\overline{\Lambda}$ particles) for pPb and PbPb data. The dominant sources of systematic uncertainties are related to the reconstruction of V^0 candidates. The systematic effects are found to have no dependence on p_T so the estimated systematic uncertainties are assumed to be constant percentages over the entire p_T range. Systematic uncertainties in v_3^{sig} are assumed to be the same as those in v_2^{sig}, as was done in Ref. [47].

Table 1
Summary of systematic uncertainties in v_n^{sig} for pPb and PbPb data.

Source	pPb (%)	PbPb (%)
V^0 mass distribution range used in fit	1	1
Size of V^0 mass region for signal	2	2
Size and location of V^0 mass sideband region	2.2	2.2
Misidentified V^0 mass region	2	2
V^0 selection criteria	3	3
Tracker misalignment	2	2
MC closure test	4	4
Trigger efficiency	2	–
Pile-up	1	–
Total	6.9	6.6

The range of the V^0 mass distributions used in fitting the signal plus background (Fig. 1) is varied by 10%. This change, which could affect the value of f^{sig} used in Eq. (7), yields a systematic uncertainty of less than 1% for the v_2^{sig} results. Changing the mass range included in the peak region could impact the values of both f^{sig} and v_2^{obs}. For a variation from $\pm 1\sigma$ to $\pm 3\sigma$, the v_2^{sig} values are found to be consistent within 2%. Systematic uncertainties due to selection of different sideband mass regions, which could change v_2^{bkg}, are estimated to be 2.2%. Possible contamination by residual misidentified V^0 candidates (i.e., K_S^0 as $\Lambda/\overline{\Lambda}$, and vice versa) is also investigated. Variation of the invariant mass range used to reject misidentified V^0 candidates leads to variations of less than 2% on v_2^{sig}. Systematic effects related to selection of the V^0 candidates are evaluated by varying the requirements on the decay length significance and $\cos\theta^{\text{point}}$, resulting in an uncertainty of 3%.

As misalignment of the tracker detector elements can affect the V^0 reconstruction performance, an alternative detector geometry is studied. Compared to the standard configuration, this alternative has the two halves of the barrel pixel detector shifted in opposite directions along the beam by a distance on the order of 100 μm. The values of v_2^{sig} found using the shifted configuration differed by less than 2% from the default ones.

To test the procedure of extracting the V^0 signal v_2 from Eq. (7), a study using EPOS LHC pPb MC events is performed to compare the extracted v_2^{sig} results with the generator-level K_S^0 and $\Lambda/\overline{\Lambda}$ values. The agreement is found to be better than 4%. Other systematic uncertainties introduced by the high-multiplicity trigger efficiency (1%) and possible residual pile-up effects (1–2%) for pPb data are estimated in the same way as in Ref. [47], and found to make only a small contribution. The various sources of systematic uncertainties are added together in quadrature to arrive at the final systematic uncertainties (6.9% for pPb and 6.6% for PbPb), which are shown as shaded boxes in Figs. 4–7.

6. Results

The 2D two-particle correlation functions measured in pPb collisions for pairs of a K_S^0 (left) and $\Lambda/\overline{\Lambda}$ (right) trigger particles and a charged associated particle ($h^\pm$) are shown in Fig. 2 in the p_T range of 1–3 GeV. The 2D correlation functions are corrected for the background V^0 candidates, following the same approach of correcting v_n in Eq. (7). The correction is negligible in this p_T range because of the high signal yield fraction of V^0 candidates. For low-multiplicity events ($N_{\text{trk}}^{\text{offline}} < 35$, Fig. 2(a) and (b)), a sharp peak near $(\Delta\eta, \Delta\phi) = (0, 0)$ due to jet fragmentation
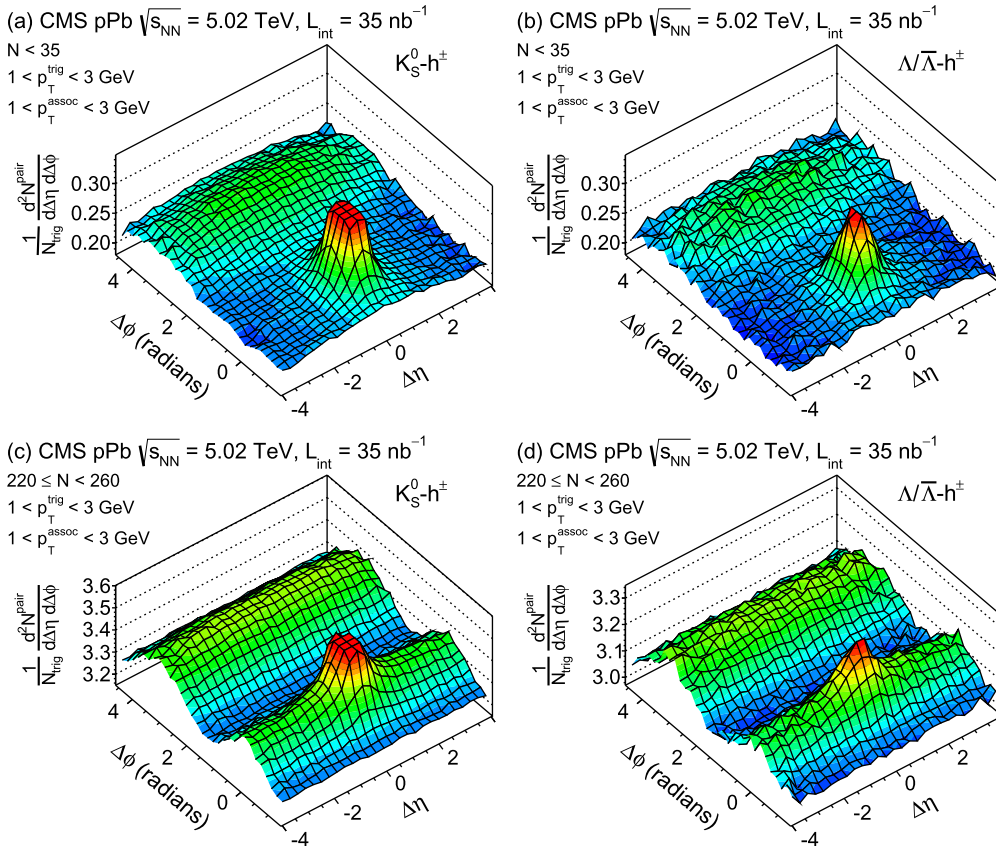

Fig. 2. The 2D two-particle correlation functions in pPb collisions at $\sqrt{s_{NN}} = 5.02$ TeV for pairs of a K_S^0 (a), (c) or $\Lambda/\overline{\Lambda}$ (b), (d) trigger particle and a charged associated particle ($h^\pm$), with $1 < p_T^{\text{trig}} < 3$ GeV and $1 < p_T^{\text{assoc}} < 3$ GeV, in the multiplicity ranges $N_{\text{trk}}^{\text{offline}} < 35$ (a), (b) and $220 \leq N_{\text{trk}}^{\text{offline}} < 260$ (c), (d). The sharp near-side peak from jet correlations is truncated to emphasize the structure outside that region.
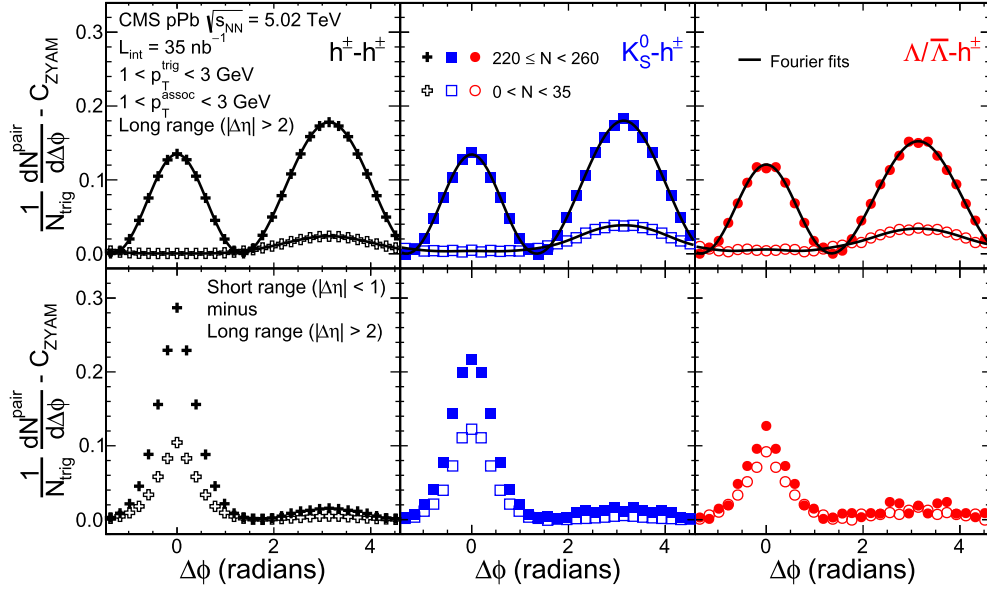
Fig. 3. The 1D $\Delta\phi$ correlation functions from pPb data after applying the ZYAM procedure, in the multiplicity range $N_{\mathrm{trk}}^{\mathrm{offline}} < 35$ (open) and $220 \leq N_{\mathrm{trk}}^{\mathrm{offline}} < 260$ (filled), for trigger particles composed of inclusive charged particles (left), K_S^0 particles (middle), and $\Lambda/\overline{\Lambda}$ particles (right). Selection of a fixed p_T^{trig} and p_T^{assoc} range of both 1–3 GeV is shown for the long-range region ($|\Delta\eta| > 2$) on top and the short-range region ($|\Delta\eta| < 1$) minus long-range region on the bottom. The curves on the top panels correspond to the Fourier fits including the first three terms. Statistical uncertainties are smaller than the size of the markers.

(truncated for better illustration of the full correlation structure) can be clearly observed for both K_S^0–$h^\pm$ and $\Lambda/\overline{\Lambda}$–$h^\pm$ correlations. Moving to high-multiplicity events ($220 \leq N_{\mathrm{trk}}^{\mathrm{offline}} < 260$, Fig. 2(c) and (d)), in addition to the peak from jet fragmentation, a pronounced long-range structure is seen at $\Delta\phi \approx 0$, extending at least 4.8 units in $|\Delta\eta|$. This structure was previously observed in high-multiplicity ($N_{\mathrm{trk}}^{\mathrm{offline}} \sim 110$) pp collisions at $\sqrt{s} = 7$ TeV [13] and pPb collisions at $\sqrt{s_{NN}} = 5.02$ TeV [14–16,47] for inclusive charged particles, and also for identified charged pions, kaons, and protons in pPb collisions at $\sqrt{s_{NN}} = 5.02$ TeV [31]. A similar long-range correlation structure has also been extensively studied in AA collisions over a wide range of energies [1–9], where it is believed to arise primarily from collective flow of a strongly interacting medium [34].

To investigate the correlation structure for different species of particles in detail, one-dimensional (1D) distributions in $\Delta\phi$ are found by averaging the signal and mixed-event 2D distributions over $|\Delta\eta| < 1$ (defined as the "short-range region") and $|\Delta\eta| > 2$ (defined as the "long-range region"), as done in Refs. [6,7,13,14,47]. Fig. 3 shows the 1D $\Delta\phi$ correlation functions from pPb data for trigger particles composed of inclusive charged particles (left) [47], K_S^0 particles (middle), and $\Lambda/\overline{\Lambda}$ particles (right), in the multiplicity range $N_{\mathrm{trk}}^{\mathrm{offline}} < 35$ (open) and $220 \leq N_{\mathrm{trk}}^{\mathrm{offline}} < 260$ (filled). The curves show the Fourier fits from Eq. (4) to the long-range region, which will be discussed in detail later. Following the standard zero-yield-at-minimum (ZYAM) procedure [47], each distribution is shifted to have zero associated yield at its minimum to represent the correlated portion of the associated yield. Selection of fixed p_T^{trig} and p_T^{assoc} ranges of 1–3 GeV is shown for the long-range region (top) and for the difference of the short- and long-range regions (bottom) in Fig. 3. As illustrated in Fig. 2, the near-side long-range signal remains nearly constant in $\Delta\eta$. Therefore, by taking a difference of 1D $\Delta\phi$ projections between the short- and long-range regions, the near-side jet correlations can be extracted. As shown in the bottom panels of Fig. 3, due to biases in multiplicity selection toward higher p_T jets, a larger jet peak yield is observed for events selected with higher multiplicities. Because charged particles are directly used in determining the multiplic-

ity in the event, this selection bias is much stronger for charged particles than K_S^0 and $\Lambda/\overline{\Lambda}$ hadrons. For $N_{\mathrm{trk}}^{\mathrm{offline}} < 35$, no near-side correlations are observed in the long-range region for any particle species. The PbPb data show qualitatively the same behavior as the pPb data, and thus are not presented here.

Recently, the v_2 anisotropy harmonics for charged pions, kaons, and protons have been studied using two-particle correlations in pPb collisions [31], and are found to be qualitatively consistent with hydrodynamic models [32,33]. In this paper, the elliptic (v_2) and triangular (v_3) flow harmonics of K_S^0 and $\Lambda/\overline{\Lambda}$ particles are extracted from the Fourier decomposition of 1D $\Delta\phi$ correlation functions for the long-range region ($|\Delta\eta| > 2$) in a significantly larger sample of pPb collisions such that the particle species dependence of v_n can be investigated in detail. In Fig. 4, the v_2^{sig} of K_S^0 and $\Lambda/\overline{\Lambda}$ particles are plotted as a function of p_T for the three lowest multiplicity ranges in PbPb and pPb collisions. These data were recorded using a minimum bias trigger. The range of the fraction of the full multiplicity distribution that each multiplicity selection corresponds to, as determined in Ref. [47], is also specified in the figure. In contrast to most other PbPb analyses, the present work uses multiplicity to classify events, instead of the total energy deposited in HF (the standard procedure of centrality determination in PbPb) [47,51]. By examining the HF energy distribution for PbPb events in each of the multiplicity ranges, the corresponding average HF fractional cross section (and its standard deviation) can be determined, which are presented for PbPb data in the figure.

In the low multiplicity region (Fig. 4), the v_2 values of K_S^0 and $\Lambda/\overline{\Lambda}$ particles are compatible within statistical uncertainties. As there is no evident long-range near-side correlation seen in these low-multiplicity events, the extracted v_2 most likely reflects back-to-back jet correlations on the away side. Away-side jet correlations typically appear as a peak structure around $\Delta\phi \approx \pi$, which contributes to various orders of Fourier terms.

The top row of Fig. 5 shows the measured v_2 values for K_S^0 and $\Lambda/\overline{\Lambda}$ particles as a function of p_T from the high multiplicity pPb data, along with the previously published results for inclusive charged particles [47]. In the $p_T \lesssim 2$ GeV region for all
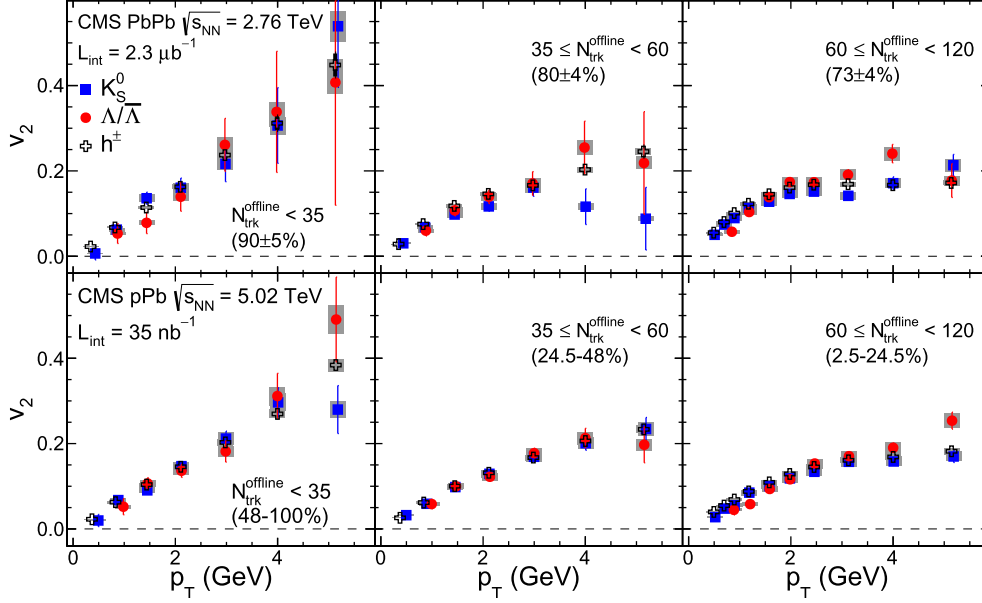
Fig. 4. The v_2 results for K^0_S (filled squares) and $\Lambda/\overline{\Lambda}$ (filled circles) particles as a function of p_T for three multiplicity ranges obtained from minimum bias triggered PbPb sample at $\sqrt{s_{NN}} = 2.76$ TeV (top row) and pPb sample at $\sqrt{s_{NN}} = 5.02$ TeV (bottom row). The error bars correspond to statistical uncertainties, while the shaded areas denote the systematic uncertainties. The values in parentheses give the mean and standard deviation of the HF fractional cross section for PbPb and the range of the fraction of the full multiplicity distribution included for pPb.

Fig. 5. Top row: the v_2 results for K^0_S (filled squares), $\Lambda/\overline{\Lambda}$ (filled circles), and inclusive charged particles (open crosses) as a function of p_T for four multiplicity ranges obtained from high-multiplicity triggered pPb sample at $\sqrt{s_{NN}} = 5.02$ TeV. Middle row: the v_2/n_q ratios for K^0_S (filled squares) and $\Lambda/\overline{\Lambda}$ (filled circles) particles as a function of KE_T/n_q, along with a fit to the K^0_S results using a polynomial function. Bottom row: ratios of v_2/n_q for K^0_S and $\Lambda/\overline{\Lambda}$ particles to the fitted polynomial function as a function of KE_T/n_q. The error bars correspond to statistical uncertainties, while the shaded areas denote the systematic uncertainties. The values in parentheses give the range of the fraction of the full multiplicity distribution included for pPb.

high-multiplicity ranges, the v_2 values of K^0_S particles are larger than those for $\Lambda/\overline{\Lambda}$ particles at each p_T value. Both of them are consistently below the v_2 values of inclusive charged particles. As most charged particles are pions, the data indicate that lighter particle species exhibit a stronger azimuthal anisotropy signal. This mass ordering behavior is consistent with expectations

in hydrodynamic models and the observation in 0–20% centrality pPb collisions [31]. A similar trend was first observed in AA collisions at RHIC [28,29]. At higher p_T, the v_2 values of $\Lambda/\overline{\Lambda}$ particles are larger than those of K^0_S. The inclusive charged particle v_2 values fall between the values of the two identified strange hadron species but are much closer to the v_2 values for K^0_S parti-
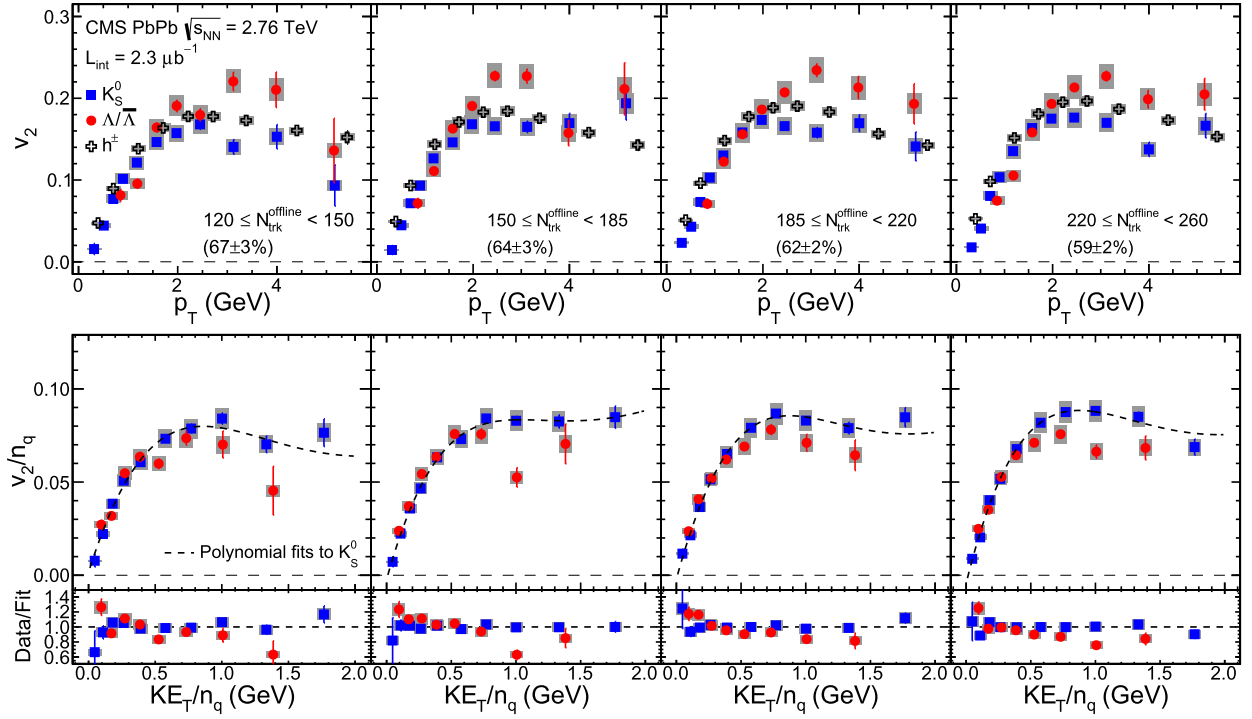
Fig. 6. Top row: the v_2 results for K_S^0 (filled squares), $\Lambda/\overline{\Lambda}$ (filled circles), and inclusive charged particles (open crosses) as a function of p_T for four multiplicity ranges obtained from minimum bias triggered PbPb sample at $\sqrt{s_{NN}} = 2.76$ TeV. Middle row: the v_2/n_q ratios for K_S^0 (filled squares) and $\Lambda/\overline{\Lambda}$ (filled circles) particles as a function of KE_T/n_q. Bottom row: ratios of v_2/n_q for K_S^0 and $\Lambda/\overline{\Lambda}$ particles to a smooth fit function of v_2/n_q for K_S^0 particles as a function of KE_T/n_q. The error bars correspond to statistical uncertainties, while the shaded areas denote the systematic uncertainties. The values in parentheses give the mean and standard deviation of the HF fractional cross section for PbPb.

cles. Note that the ratio of baryon to meson yield in pPb collisions is enhanced at higher p_T, an effect that becomes stronger as multiplicity increases [54,55]. This should also be taken into account when comparing v_n values between inclusive and identified particles. Comparing the results in Fig. 4 and Fig. 5, the dependence of v_2 on the particle species may already be emerging in the multiplicity range of $60 \leq N_{trk}^{offline} < 120$.

The scaling behavior of v_2 divided by the number of constituent quarks as a function of transverse kinetic energy per quark, KE_T/n_q, is investigated for high-multiplicity pPb events in the middle row of Fig. 5. After scaling by the number of quarks, the v_2 distributions for K_S^0 and $\Lambda/\overline{\Lambda}$ particles are found to be in agreement. The middle row of Fig. 5 also shows the result of fitting a polynomial function to the K_S^0 data. The bottom row of Fig. 5 shows the n_q-scaled v_2 results for K_S^0 and $\Lambda/\overline{\Lambda}$ particles divided by this polynomial function fit, indicating that the scaling is valid to better than 10% over most of the KE_T/n_q range, except for $KE_T/n_q < 0.2$ GeV where the deviation grows to about 20%. In AA collisions, this approximate scaling behavior is conjectured to be related to quark recombination [39–41], which postulates that collective flow is developed among constituent quarks before they combine into final-state hadrons. Note that the scaling of v_2 with the number of constituent quarks was originally observed as a function of p_T, instead of KE_T, for the intermediate p_T range of a few GeV [38], and interpreted in a simple picture of quark coalescence [39]. However, it was later discovered that when plotted as a function of KE_T in order to remove the mass difference of identified hadrons, the scaling appears to hold over the entire kinematic range [42,43]. However, this scaling behavior is not expected to be exact at low p_T in hydrodynamic models because of the impact of radial flow. As the v_n data tend to approach a constant value as a function of p_T or KE_T for $p_T \gtrsim 2$ GeV, the scaling behavior in terms

of p_T and KE_T cannot be differentiated in that regime. Therefore, the n_q-scaled v_n results in this paper are presented as a function of KE_T/n_q in order to explore the scaling behavior over a wider kinematic range.

The particle species dependence of v_2 and its scaling behavior is also studied in PbPb data over the same multiplicity ranges as for the pPb data, as shown in Fig. 6. The mean and standard deviation of the HF fractional cross section of the PbPb data are indicated on the plots. Qualitatively, a similar particle-species dependence of v_2 is observed. However, the mass ordering effect is found to be less evident in PbPb data than in pPb data for all multiplicity ranges. In hydrodynamic models, this may indicate a stronger radial flow is developed in the pPb system as its energy density is higher than that of a PbPb system due to having a smaller size system at the same multiplicity. Moreover, the n_q-scaled v_2 data in PbPb at similar multiplicities suggest a stronger violation of constituent quark number scaling, up to 25%, than is observed in pPb, especially for higher KE_T/n_q values. This is also observed in peripheral AuAu collisions at RHIC, while the scaling applies more closely for central AuAu collisions [56].

The triangular flow harmonic, v_3, of K_S^0 and $\Lambda/\overline{\Lambda}$ particles is also extracted in pPb and PbPb collisions, as shown in Fig. 7. Due to limited statistical precision, only the result in the multiplicity range $185 \leq N_{trk}^{offline} < 350$ is presented. A similar species dependence of v_3 to that of v_2 is observed and, within the statistical uncertainties, the v_3 values scaled by the constituent quark number for K_S^0 and $\Lambda/\overline{\Lambda}$ particles match at the level of 20% over the full KE_T/n_q range. To date, no calculations of the quark number scaling of triangular flow, v_3, have been performed in the parton recombination model.
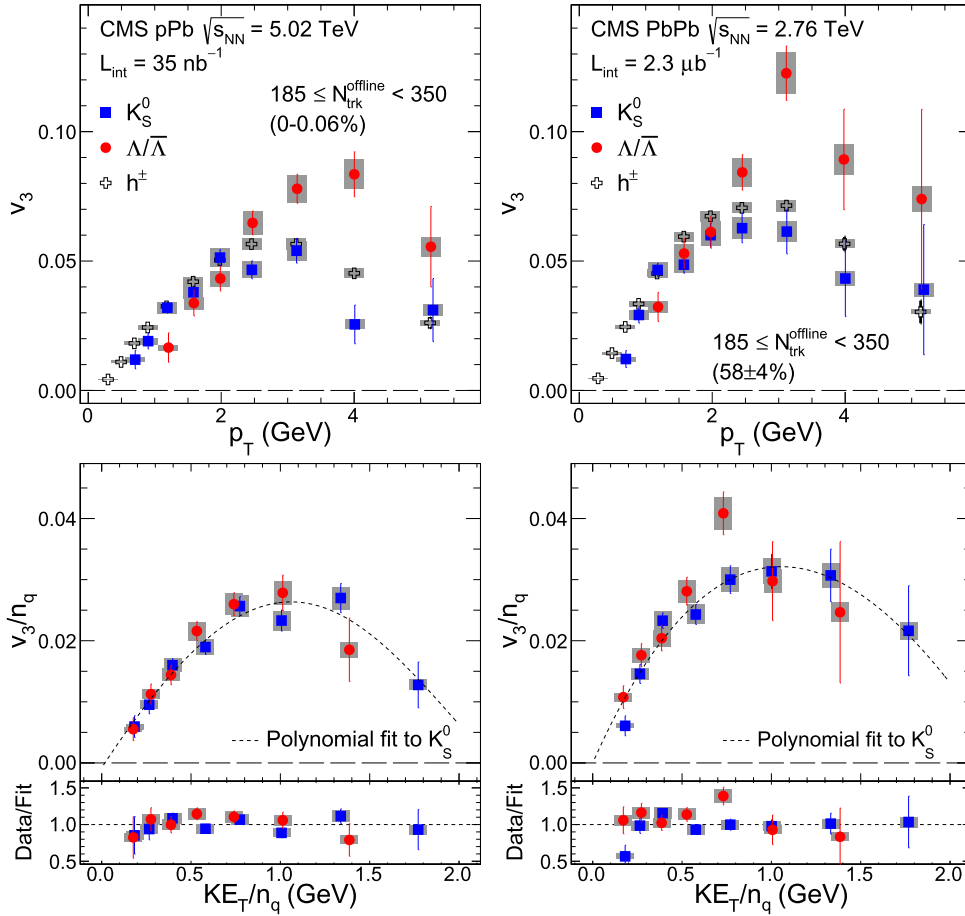
Fig. 7. Top: the v_3 results for K_S^0 (filled squares), $\Lambda/\overline{\Lambda}$ (filled circles), and inclusive charged particles (open crosses) as a function of p_T for the multiplicity range $185 \leq N_{trk}^{offline} < 350$ in pPb collisions at $\sqrt{s_{NN}} = 5.02$ TeV (left) and in PbPb collisions at $\sqrt{s_{NN}} = 2.76$ TeV (right). Bottom: the n_q-scaled v_3 values of K_S^0 (filled squares) and $\Lambda/\overline{\Lambda}$ (filled circles) particles as a function of KE_T/n_q for the same two systems. Ratios of v_n/n_q to a smooth fit function of v_n/n_q for K_S^0 particles as a function of KE_T/n_q are also shown. The error bars correspond to statistical uncertainties, while the shaded areas denote the systematic uncertainties. The values in parentheses give the mean and standard deviation of the HF fractional cross section for PbPb and the range of the fraction of the full multiplicity distribution included for pPb.

7. Summary

Measurements of two-particle correlations with an identified K_S^0 or $\Lambda/\overline{\Lambda}$ trigger particle have been presented over a broad transverse momentum and pseudorapidity range in pPb collisions at $\sqrt{s_{NN}} = 5.02$ TeV and PbPb collisions at $\sqrt{s_{NN}} = 2.76$ TeV. With the implementation of a high-multiplicity trigger during the LHC 2013 pPb run, the identified particle correlation data in pPb collisions are explored over a broad particle multiplicity range, comparable to that covered by 50–100% centrality PbPb collisions. The long-range ($|\Delta\eta| > 2$) correlations are quantified in terms of azimuthal anisotropy Fourier harmonics (v_n) motivated by hydrodynamic models. In low-multiplicity pPb and PbPb events, similar v_2 values of K_S^0 and $\Lambda/\overline{\Lambda}$ particles are observed, which likely originate from back-to-back jet correlations. For higher event multiplicities, a particle species dependence of $v_2(p_T)$ and $v_3(p_T)$ is observed. For $p_T \lesssim 2$ GeV, the values of v_n for K_S^0 particles are found to be larger than those of $\Lambda/\overline{\Lambda}$ particles, while this order is reversed at higher p_T. This behavior is consistent with RHIC and LHC results in AA collisions and for identified charged hadrons in pPb and dAu collisions. For similar event multiplicities, the particle species dependence of v_2 and v_3 at low p_T is observed to be more pronounced in pPb than in PbPb collisions. In the context of hydrodynamic models, this may indicate that a stronger radial flow boost is developed in pPb collisions. Furthermore, constituent quark number scaling of v_2 and v_3 between K_S^0 and $\Lambda/\overline{\Lambda}$ parti-

cles is found to apply for PbPb and high-multiplicity pPb events. The constituent quark number scaling is found to hold at the 10% (25%) level in pPb (PbPb) collisions, for similar event multiplicities. It will be interesting to see if this scaling law continues to hold for other particles. The results presented in this paper provide important input to the further exploration of the possible collective flow origin of long-range correlations, and can be used to evaluate models of quark recombination in a deconfined medium of quarks and gluons.

References

[1] J. Adams, et al., STAR Collaboration, Distributions of charged hadrons associated with high transverse momentum particles in pp and Au + Au collisions at $\sqrt{s_{NN}} = 200$ GeV, Phys. Rev. Lett. 95 (2005) 152301, http://dx.doi.org/10.1103/PhysRevLett.95.152301, arXiv:nucl-ex/0501016.

[2] B.I. Abelev, et al., STAR Collaboration, Long range rapidity correlations and jet production in high energy nuclear collisions, Phys. Rev. C 80 (2009) 064912, http://dx.doi.org/10.1103/PhysRevC.80.064912, arXiv:0909.0191.

[3] B. Alver, et al., PHOBOS Collaboration, System size dependence of cluster properties from two-particle angular correlations in Cu + Cu and Au + Au collisions at $\sqrt{s_{NN}} = 200$ GeV, Phys. Rev. C 81 (2010) 024904, http://dx.doi.org/10.1103/PhysRevC.81.024904, arXiv:0812.1172.

[4] B. Alver, et al., PHOBOS Collaboration, High transverse momentum triggered correlations over a large pseudorapidity acceptance in Au + Au collisions at $\sqrt{s_{NN}} = 200$ GeV, Phys. Rev. Lett. 104 (2010) 062301, http://dx.doi.org/10.1103/PhysRevLett.104.062301, arXiv:0903.2811.

[5] B.I. Abelev, et al., STAR Collaboration, Three-particle coincidence of the long range pseudorapidity correlation in high energy nucleus–nucleus collisions, Phys. Rev. Lett. 105 (2010) 022301, http://dx.doi.org/10.1103/PhysRevLett.105.022301, arXiv:0912.3977.

[6] CMS Collaboration, Long-range and short-range dihadron angular correlations in central PbPb collisions at $\sqrt{s_{NN}} = 2.76$ TeV, J. High Energy Phys. 07 (2011) 076, http://dx.doi.org/10.1007/JHEP07(2011)076, arXiv:1105.2438.

[7] CMS Collaboration, Centrality dependence of dihadron correlations and azimuthal anisotropy harmonics in PbPb collisions at $\sqrt{s_{NN}} = 2.76$ TeV, Eur. Phys. J. C 72 (2012) 2012, http://dx.doi.org/10.1140/epjc/s10052-012-2012-3, arXiv:1201.3158.

[8] ALICE Collaboration, Harmonic decomposition of two-particle angular correlations in Pb–Pb collisions at $\sqrt{s_{NN}} = 2.76$ TeV, Phys. Lett. B 708 (2012) 249, http://dx.doi.org/10.1016/j.physletb.2012.01.060, arXiv:1109.2501.

[9] ATLAS Collaboration, Measurement of the azimuthal anisotropy for charged particle production in $\sqrt{s_{NN}} = 2.76$ TeV lead–lead collisions with the ATLAS detector, Phys. Rev. C 86 (2012) 014907, http://dx.doi.org/10.1103/PhysRevC.86.014907, arXiv:1203.3087.

[10] CMS Collaboration, Studies of azimuthal dihadron correlations in ultra-central PbPb collisions at $\sqrt{s_{NN}} = 2.76$ TeV, J. High Energy Phys. 02 (2014) 088, http://dx.doi.org/10.1007/JHEP02(2014)088, arXiv:1312.1845.

[11] J.-Y. Ollitrault, Anisotropy as a signature of transverse collective flow, Phys. Rev. D 46 (1992) 229, http://dx.doi.org/10.1103/PhysRevD.46.229.

[12] B. Alver, G. Roland, Collision geometry fluctuations and triangular flow in heavy-ion collisions, Phys. Rev. C 81 (2010) 054905, http://dx.doi.org/10.1103/PhysRevC.81.054905, arXiv:1003.0194.

[13] CMS Collaboration, Observation of long-range near-side angular correlations in proton–proton collisions at the LHC, J. High Energy Phys. 09 (2010) 091, http://dx.doi.org/10.1007/JHEP09(2010)091, arXiv:1009.4122.

[14] CMS Collaboration, Observation of long-range near-side angular correlations in pPb collisions at the LHC, Phys. Lett. B 718 (2013) 795, http://dx.doi.org/10.1016/j.physletb.2012.11.025, arXiv:1210.5482.

[15] ALICE Collaboration, Long-range angular correlations on the near and away side in pPb collisions at $\sqrt{s_{NN}} = 5.02$ TeV, Phys. Lett. B 719 (2013) 29, http://dx.doi.org/10.1016/j.physletb.2013.01.012, arXiv:1212.2001.

[16] ATLAS Collaboration, Observation of associated near-side and away-side long-range correlations in $\sqrt{s_{NN}} = 5.02$ TeV proton–lead collisions with the ATLAS detector, Phys. Rev. Lett. 110 (2013) 182302, http://dx.doi.org/10.1103/PhysRevLett.110.182302, arXiv:1212.5198.

[17] A. Adare, et al., PHENIX Collaboration, Measurement of long-range angular correlation and quadrupole anisotropy of pions and (anti)protons in central d + Au collisions at $\sqrt{s_{NN}} = 200$ GeV, arXiv:1404.7461, 2014.

[18] W. Li, Observation of a ridge correlation structure in high multiplicity proton–proton collisions: a brief review, Mod. Phys. Lett. A 27 (2012) 1230018, http://dx.doi.org/10.1142/S0217732312300182, arXiv:1206.0148.

[19] P. Bożek, Collective flow in p–Pb and d–Pd collisions at TeV energies, Phys. Rev. C 85 (2012) 014911, http://dx.doi.org/10.1103/PhysRevC.85.014911, arXiv:1112.0915.

[20] P. Bożek, W. Broniowski, Correlations from hydrodynamic flow in pPb collisions, Phys. Lett. B 718 (2013) 1557, http://dx.doi.org/10.1016/j.physletb.2012.12.051, arXiv:1211.0845.

[21] K. Dusling, R. Venugopalan, Explanation of systematics of CMS p + Pb high multiplicity dihadron data at $\sqrt{s_{NN}} = 5.02$ TeV, Phys. Rev. D 87 (2013) 054014, http://dx.doi.org/10.1103/PhysRevD.87.054014, arXiv:1211.3701.

[22] K. Dusling, R. Venugopalan, Evidence for BFKL and saturation dynamics from dihadron spectra at the LHC, Phys. Rev. D 87 (2013) 051502, http://dx.doi.org/10.1103/PhysRevD.87.051502, arXiv:1210.3890.

[23] P. Huovinen, P.F. Kolb, U.W. Heinz, P.V. Ruuskanen, S.A. Voloshin, Radial and elliptic flow at RHIC: further predictions, Phys. Lett. B 503 (2001) 58, http://dx.doi.org/10.1016/S0370-2693(01)00219-2, arXiv:hep-ph/0101136.

[24] P.F. Kolb, U.W. Heinz, Hydrodynamic description of ultrarelativistic heavy-ion collisions, in: R.C. Hwa, X.N. Wang (Eds.), Quark Gluon Plasma 3, World Scientific, Singapore, 2003, p. 634, arXiv:nucl-th/0305084.

[25] C. Shen, U. Heinz, P. Huovinen, H. Song, Radial and elliptic flow in Pb + Pb collisions at energies available at the CERN Large Hadron Collider from viscous hydrodynamics, Phys. Rev. C 84 (2011) 044903, http://dx.doi.org/10.1103/PhysRevC.84.044903, arXiv:1105.3226.

[26] J. Adams, et al., STAR Collaboration, Experimental and theoretical challenges in the search for the quark gluon plasma: the STAR Collaboration's critical assessment of the evidence from RHIC collisions, Nucl. Phys. A 757 (2005) 102, http://dx.doi.org/10.1016/j.nuclphysa.2005.03.085, arXiv:nucl-ex/0501009.

[27] K. Adcox, et al., PHENIX Collaboration, Formation of dense partonic matter in relativistic nucleus–nucleus collisions at RHIC: experimental evaluation by the PHENIX Collaboration, Nucl. Phys. A 757 (2005) 184, http://dx.doi.org/10.1016/j.nuclphysa.2005.03.086, arXiv:nucl-ex/0410003.

[28] S.S. Adler, et al., PHENIX Collaboration, Elliptic flow of identified hadrons in Au + Au collisions at $\sqrt{s_{NN}} = 200$ GeV, Phys. Rev. Lett. 91 (2003) 182301, http://dx.doi.org/10.1103/PhysRevLett.91.182301, arXiv:nucl-ex/0305013.

[29] C. Adler, et al., STAR Collaboration, Identified particle elliptic flow in Au + Au collisions at $\sqrt{s_{NN}} = 130$ GeV, Phys. Rev. Lett. 87 (2001) 182301, http://dx.doi.org/10.1103/PhysRevLett.87.182301, arXiv:nucl-ex/0107003.

[30] ALICE Collaboration, Elliptic flow of identified hadrons in Pb–Pb collisions at $\sqrt{s_{NN}} = 2.76$ TeV, arXiv:1405.4632, 2014.

[31] ALICE Collaboration, Long-range angular correlations of π, K and p in p–Pb collisions at $\sqrt{s_{NN}} = 5.02$ TeV, Phys. Lett. B 726 (2013) 164, http://dx.doi.org/10.1016/j.physletb.2013.08.024, arXiv:1307.3237.

[32] K. Werner, M. Bleicher, B. Guiot, I. Karpenko, T. Pierog, Evidence for flow from hydrodynamic simulations of pPb collisions at 5.02 TeV from v_2 mass splitting, Phys. Rev. Lett. 112 (2014) 232301, http://dx.doi.org/10.1103/PhysRevLett.112.232301, arXiv:1307.4379.

[33] P. Bożek, W. Broniowski, G. Torrieri, Mass hierarchy in identified particle distributions in proton–lead collisions, Phys. Rev. Lett. 111 (2013) 172303, http://dx.doi.org/10.1103/PhysRevLett.111.172303, arXiv:1307.5060.

[34] S. Voloshin, Y. Zhang, Flow study in relativistic nuclear collisions by Fourier expansion of azimuthal particle distributions, Z. Phys. C 70 (1996) 665, http://dx.doi.org/10.1007/s002880050141, arXiv:hep-ph/9407282.

[35] B.H. Alver, C. Gombeaud, M. Luzum, J.-Y. Ollitrault, Triangular flow in hydrodynamics and transport theory, Phys. Rev. C 82 (2010) 034913, http://dx.doi.org/10.1103/PhysRevC.82.034913, arXiv:1007.5469.

[36] B. Schenke, S. Jeon, C. Gale, Elliptic and triangular flow in event-by-event $D = 3 + 1$ viscous hydrodynamics, Phys. Rev. Lett. 106 (2011) 042301, http://dx.doi.org/10.1103/PhysRevLett.106.042301, arXiv:1009.3244.

[37] Z. Qiu, C. Shen, U. Heinz, Hydrodynamic elliptic and triangular flow in Pb–Pb collisions at $\sqrt{s_{NN}} = 2.76A$ TeV, Phys. Lett. B 707 (2012) 151, http://dx.doi.org/10.1016/j.physletb.2011.12.041, arXiv:1110.3033.

[38] J. Adams, et al., STAR Collaboration, Particle type dependence of azimuthal anisotropy and nuclear modification of particle production in Au + Au collisions at $\sqrt{s_{NN}} = 200$ GeV, Phys. Rev. Lett. 92 (2004) 052302, http://dx.doi.org/10.1103/PhysRevLett.92.052302, arXiv:nucl-ex/0306007.

[39] D. Molnar, S.A. Voloshin, Elliptic flow at large transverse momenta from quark coalescence, Phys. Rev. Lett. 91 (2003) 092301, http://dx.doi.org/10.1103/PhysRevLett.91.092301, arXiv:nucl-th/0302014.

[40] V. Greco, C.M. Ko, P. Levai, Parton coalescence and the anti-proton/pion anomaly at RHIC, Phys. Rev. Lett. 90 (2003) 202302, http://dx.doi.org/10.1103/PhysRevLett.90.202302, arXiv:nucl-th/0301093.

[41] R.J. Fries, B. Muller, C. Nonaka, S.A. Bass, Hadronization in heavy ion collisions: recombination and fragmentation of partons, Phys. Rev. Lett. 90 (2003) 202303, http://dx.doi.org/10.1103/PhysRevLett.90.202303, arXiv:nucl-th/0301087.

[42] B.I. Abelev, et al., STAR Collaboration, Mass, quark-number, and $\sqrt{s_{NN}}$ dependence of the second and fourth flow harmonics in ultra-relativistic nucleus–nucleus collisions, Phys. Rev. C 75 (2007) 054906, http://dx.doi.org/10.1103/PhysRevC.75.054906, arXiv:nucl-ex/0701010.

[43] A. Adare, et al., PHENIX Collaboration, Scaling properties of azimuthal anisotropy in Au + Au and Cu + Cu collisions at $\sqrt{s_{NN}} = 200$ GeV, Phys. Rev. Lett. 98 (2007) 162301, http://dx.doi.org/10.1103/PhysRevLett.98.162301, arXiv:nucl-ex/0608033.

[44] CMS Collaboration, The CMS experiment at the CERN LHC, J. Instrum. 3 (2008) S08004, http://dx.doi.org/10.1088/1748-0221/3/08/S08004.

[45] S. Agostinelli, et al., Geant4 Collaboration, Geant4—a simulation toolkit, Nucl. Instrum. Methods Phys. Res., Sect. A, Accel. Spectrom. Detect. Assoc. Equip. 506 (2003) 250, http://dx.doi.org/10.1016/S0168-9002(03)01368-8.

[46] CMS Collaboration, Luminosity calibration for the 2013 proton–lead and proton–proton data taking, CMS Physics Analysis Summary CMS-PAS-LUM-13–002 2014, https://cds.cern.ch/record/1643269.

[47] S. Chatrchyan, et al., CMS Collaboration, Multiplicity and transverse momentum dependence of two- and four-particle correlations in pPb and PbPb collisions, Phys. Lett. B 724 (2013) 213, http://dx.doi.org/10.1016/j.physletb.2013.06.028, arXiv:1305.0609.

[48] CMS Collaboration, Description and performance of track and primary-vertex reconstruction with the CMS tracker, arXiv:1405.6569, 2014.

[49] T. Pierog, I. Karpenko, J.M. Katzy, E. Yatsenko, K. Werner, EPOS LHC: test of collective hadronization with LHC data, arXiv:1306.0121, 2013.

[50] M. Gyulassy, X.-N. Wang, HIJING 1.0: a Monte Carlo program for parton and particle production in high-energy hadronic and nuclear collisions, Comput. Phys. Commun. 83 (1994) 307, http://dx.doi.org/10.1016/0010-4655(94)90057-4, arXiv:nucl-th/9502021.

[51] CMS Collaboration, Azimuthal anisotropy of charged particles at high transverse momenta in PbPb collisions at $\sqrt{s_{NN}} = 2.76$ TeV, Phys. Rev. Lett. 109 (2012) 022301, http://dx.doi.org/10.1103/PhysRevLett.109.022301, arXiv:1204.1850.

[52] CMS Collaboration, Strange particle production in pp collisions at $\sqrt{s} = 0.9$ and 7 TeV, J. High Energy Phys. 05 (2011) 064, http://dx.doi.org/10.1007/JHEP05(2011)064, arXiv:1102.4282.

[53] J. Beringer, et al., Particle Data Group, Review of Particle Physics (RPP), Phys. Rev. D 86 (2012) 010001, http://dx.doi.org/10.1103/PhysRevD.86.010001.

[54] CMS Collaboration, Study of the production of charged pions, kaons, and protons in pPb collisions at $\sqrt{s_{NN}} = 5.02$ TeV, Eur. Phys. J. C 72 (2013) 2012, http://dx.doi.org/10.1140/epjc/s10052-014-2847-x, arXiv:1307.3442.

[55] ALICE Collaboration, Multiplicity dependence of pion, kaon, proton and Lambda production in p–Pb collisions at $\sqrt{s_{NN}} = 5.02$ TeV, Phys. Lett. B 728 (2014) 25, http://dx.doi.org/10.1016/j.physletb.2013.11.020, arXiv:1307.6796.

[56] A. Adare, et al., PHENIX Collaboration, Deviation from quark-number scaling of the anisotropy parameter v_2 of pions, kaons, and protons in Au + Au collisions at $\sqrt{s_{NN}} = 200$ GeV, Phys. Rev. C 85 (2012) 064914, http://dx.doi.org/10.1103/PhysRevC.85.064914, arXiv:1203.2644.

CMS Collaboration

V. Khachatryan, A.M. Sirunyan, A. Tumasyan

Yerevan Physics Institute, Yerevan, Armenia

W. Adam, T. Bergauer, M. Dragicevic, J. Erö, C. Fabjan [1], M. Friedl, R. Frühwirth [1], V.M. Ghete, C. Hartl, N. Hörmann, J. Hrubec, M. Jeitler [1], W. Kiesenhofer, V. Knünz, M. Krammer [1], I. Krätschmer, D. Liko, I. Mikulec, D. Rabady [2], B. Rahbaran, H. Rohringer, R. Schöfbeck, J. Strauss, A. Taurok, W. Treberer-Treberspurg, W. Waltenberger, C.-E. Wulz [1]

Institut für Hochenergiephysik der OeAW, Wien, Austria

V. Mossolov, N. Shumeiko, J. Suarez Gonzalez

National Centre for Particle and High Energy Physics, Minsk, Belarus

S. Alderweireldt, M. Bansal, S. Bansal, T. Cornelis, E.A. De Wolf, X. Janssen, A. Knutsson, S. Luyckx, S. Ochesanu, R. Rougny, M. Van De Klundert, H. Van Haevermaet, P. Van Mechelen, N. Van Remortel, A. Van Spilbeeck

Universiteit Antwerpen, Antwerpen, Belgium

F. Blekman, S. Blyweert, J. D'Hondt, N. Daci, N. Heracleous, J. Keaveney, S. Lowette, M. Maes, A. Olbrechts, Q. Python, D. Strom, S. Tavernier, W. Van Doninck, P. Van Mulders, G.P. Van Onsem, I. Villella

Vrije Universiteit Brussel, Brussel, Belgium

C. Caillol, B. Clerbaux, G. De Lentdecker, D. Dobur, L. Favart, A.P.R. Gay, A. Grebenyuk, A. Léonard, A. Mohammadi, L. Perniè [2], T. Reis, T. Seva, L. Thomas, C. Vander Velde, P. Vanlaer, J. Wang, F. Zenoni

Université Libre de Bruxelles, Bruxelles, Belgium

V. Adler, K. Beernaert, L. Benucci, A. Cimmino, S. Costantini, S. Crucy, S. Dildick, A. Fagot, G. Garcia, J. Mccartin, A.A. Ocampo Rios, D. Ryckbosch, S. Salva Diblen, M. Sigamani, N. Strobbe, F. Thyssen, M. Tytgat, E. Yazgan, N. Zaganidis

Ghent University, Ghent, Belgium

S. Basegmez, C. Beluffi [3], G. Bruno, R. Castello, A. Caudron, L. Ceard, G.G. Da Silveira, C. Delaere, T. du Pree, D. Favart, L. Forthomme, A. Giammanco [4], J. Hollar, A. Jafari, P. Jez, M. Komm, V. Lemaitre, C. Nuttens, D. Pagano, L. Perrini, A. Pin, K. Piotrzkowski, A. Popov [5], L. Quertenmont, M. Selvaggi, M. Vidal Marono, J.M. Vizan Garcia

Université Catholique de Louvain, Louvain-la-Neuve, Belgium

N. Beliy, T. Caebergs, E. Daubie, G.H. Hammad

Université de Mons, Mons, Belgium

W.L. Aldá Júnior, G.A. Alves, L. Brito, M. Correa Martins Junior, T. Dos Reis Martins, C. Mora Herrera, M.E. Pol

Centro Brasileiro de Pesquisas Fisicas, Rio de Janeiro, Brazil

W. Carvalho, J. Chinellato [6], A. Custódio, E.M. Da Costa, D. De Jesus Damiao, C. De Oliveira Martins, S. Fonseca De Souza, H. Malbouisson, D. Matos Figueiredo, L. Mundim, H. Nogima, W.L. Prado Da Silva, J. Santaolalla, A. Santoro, A. Sznajder, E.J. Tonelli Manganote [6], A. Vilela Pereira

Universidade do Estado do Rio de Janeiro, Rio de Janeiro, Brazil

C.A. Bernardes [b], S. Dogra [a], T.R. Fernandez Perez Tomei [a], E.M. Gregores [b], P.G. Mercadante [b], S.F. Novaes [a], Sandra S. Padula [a]

[a] *Universidade Estadual Paulista, São Paulo, Brazil*
[b] *Universidade Federal do ABC, São Paulo, Brazil*

A. Aleksandrov, V. Genchev [2], P. Iaydjiev, A. Marinov, S. Piperov, M. Rodozov, S. Stoykova, G. Sultanov, V. Tcholakov, M. Vutova

Institute for Nuclear Research and Nuclear Energy, Sofia, Bulgaria

A. Dimitrov, I. Glushkov, R. Hadjiiska, V. Kozhuharov, L. Litov, B. Pavlov, P. Petkov

University of Sofia, Sofia, Bulgaria

J.G. Bian, G.M. Chen, H.S. Chen, M. Chen, R. Du, C.H. Jiang, R. Plestina [7], J. Tao, Z. Wang

Institute of High Energy Physics, Beijing, China

C. Asawatangtrakuldee, Y. Ban, S. Liu, Y. Mao, S.J. Qian, D. Wang, L. Zhang, W. Zou

State Key Laboratory of Nuclear Physics and Technology, Peking University, Beijing, China

C. Avila, L.F. Chaparro Sierra, C. Florez, J.P. Gomez, B. Gomez Moreno, J.C. Sanabria

Universidad de Los Andes, Bogota, Colombia

N. Godinovic, D. Lelas, D. Polic, I. Puljak

University of Split, Faculty of Electrical Engineering, Mechanical Engineering and Naval Architecture, Split, Croatia

Z. Antunovic, M. Kovac

University of Split, Faculty of Science, Split, Croatia

V. Brigljevic, K. Kadija, J. Luetic, D. Mekterovic, L. Sudic

Institute Rudjer Boskovic, Zagreb, Croatia

A. Attikis, G. Mavromanolakis, J. Mousa, C. Nicolaou, F. Ptochos, P.A. Razis

University of Cyprus, Nicosia, Cyprus

M. Bodlak, M. Finger, M. Finger Jr. [8]

Charles University, Prague, Czech Republic

Y. Assran [9], A. Ellithi Kamel [10], M.A. Mahmoud [11], A. Radi [12,13]

Academy of Scientific Research and Technology of the Arab Republic of Egypt, Egyptian Network of High Energy Physics, Cairo, Egypt

M. Kadastik, M. Murumaa, M. Raidal, A. Tiko

National Institute of Chemical Physics and Biophysics, Tallinn, Estonia

P. Eerola, G. Fedi, M. Voutilainen

Department of Physics, University of Helsinki, Helsinki, Finland

J. Härkönen, V. Karimäki, R. Kinnunen, M.J. Kortelainen, T. Lampén, K. Lassila-Perini, S. Lehti, T. Lindén, P. Luukka, T. Mäenpää, T. Peltola, E. Tuominen, J. Tuominiemi, E. Tuovinen, L. Wendland

Helsinki Institute of Physics, Helsinki, Finland

J. Talvitie, T. Tuuva

Lappeenranta University of Technology, Lappeenranta, Finland

M. Besancon, F. Couderc, M. Dejardin, D. Denegri, B. Fabbro, J.L. Faure, C. Favaro, F. Ferri, S. Ganjour, A. Givernaud, P. Gras, G. Hamel de Monchenault, P. Jarry, E. Locci, J. Malcles, J. Rander, A. Rosowsky, M. Titov

DSM/IRFU, CEA/Saclay, Gif-sur-Yvette, France

S. Baffioni, F. Beaudette, P. Busson, C. Charlot, T. Dahms, M. Dalchenko, L. Dobrzynski, N. Filipovic, A. Florent, R. Granier de Cassagnac, L. Mastrolorenzo, P. Miné, C. Mironov, I.N. Naranjo, M. Nguyen, C. Ochando, P. Paganini, S. Regnard, R. Salerno, J.B. Sauvan, Y. Sirois, C. Veelken, Y. Yilmaz, A. Zabi

Laboratoire Leprince-Ringuet, Ecole Polytechnique, IN2P3-CNRS, Palaiseau, France

J.-L. Agram [14], J. Andrea, A. Aubin, D. Bloch, J.-M. Brom, E.C. Chabert, C. Collard, E. Conte [14], J.-C. Fontaine [14], D. Gelé, U. Goerlach, C. Goetzmann, A.-C. Le Bihan, P. Van Hove

Institut Pluridisciplinaire Hubert Curien, Université de Strasbourg, Université de Haute Alsace Mulhouse, CNRS/IN2P3, Strasbourg, France

S. Gadrat

Centre de Calcul de l'Institut National de Physique Nucleaire et de Physique des Particules, CNRS/IN2P3, Villeurbanne, France

S. Beauceron, N. Beaupere, G. Boudoul [2], E. Bouvier, S. Brochet, C.A. Carrillo Montoya, J. Chasserat, R. Chierici, D. Contardo [2], P. Depasse, H. El Mamouni, J. Fan, J. Fay, S. Gascon, M. Gouzevitch, B. Ille, T. Kurca, M. Lethuillier, L. Mirabito, S. Perries, J.D. Ruiz Alvarez, D. Sabes, L. Sgandurra, V. Sordini, M. Vander Donckt, P. Verdier, S. Viret, H. Xiao

Université de Lyon, Université Claude Bernard Lyon 1, CNRS-IN2P3, Institut de Physique Nucléaire de Lyon, Villeurbanne, France

Z. Tsamalaidze [8]

Institute of High Energy Physics and Informatization, Tbilisi State University, Tbilisi, Georgia

C. Autermann, S. Beranek, M. Bontenackels, M. Edelhoff, L. Feld, O. Hindrichs, K. Klein, A. Ostapchuk, A. Perieanu, F. Raupach, J. Sammet, S. Schael, H. Weber, B. Wittmer, V. Zhukov [5]

RWTH Aachen University, I. Physikalisches Institut, Aachen, Germany

M. Ata, M. Brodski, E. Dietz-Laursonn, D. Duchardt, M. Erdmann, R. Fischer, A. Güth, T. Hebbeker, C. Heidemann, K. Hoepfner, D. Klingebiel, S. Knutzen, P. Kreuzer, M. Merschmeyer, A. Meyer, P. Millet, M. Olschewski, K. Padeken, P. Papacz, H. Reithler, S.A. Schmitz, L. Sonnenschein, D. Teyssier, S. Thüer, M. Weber

RWTH Aachen University, III. Physikalisches Institut A, Aachen, Germany

V. Cherepanov, Y. Erdogan, G. Flügge, H. Geenen, M. Geisler, W. Haj Ahmad, A. Heister, F. Hoehle, B. Kargoll, T. Kress, Y. Kuessel, A. Künsken, J. Lingemann [2], A. Nowack, I.M. Nugent, L. Perchalla, O. Pooth, A. Stahl

RWTH Aachen University, III. Physikalisches Institut B, Aachen, Germany

I. Asin, N. Bartosik, J. Behr, W. Behrenhoff, U. Behrens, A.J. Bell, M. Bergholz [15], A. Bethani, K. Borras, A. Burgmeier, A. Cakir, L. Calligaris, A. Campbell, S. Choudhury, F. Costanza, C. Diez Pardos, S. Dooling, T. Dorland, G. Eckerlin, D. Eckstein, T. Eichhorn, G. Flucke, J. Garay Garcia, A. Geiser, P. Gunnellini, J. Hauk, M. Hempel [15], D. Horton, H. Jung, A. Kalogeropoulos, M. Kasemann, P. Katsas, J. Kieseler, C. Kleinwort, D. Krücker, W. Lange, J. Leonard, K. Lipka, A. Lobanov, W. Lohmann [15], B. Lutz, R. Mankel, I. Marfin [15], I.-A. Melzer-Pellmann, A.B. Meyer, G. Mittag, J. Mnich, A. Mussgiller, S. Naumann-Emme, A. Nayak, O. Novgorodova, E. Ntomari, H. Perrey, D. Pitzl, R. Placakyte, A. Raspereza, P.M. Ribeiro Cipriano, B. Roland, E. Ron, M.Ö. Sahin, J. Salfeld-Nebgen, P. Saxena, R. Schmidt [15], T. Schoerner-Sadenius, M. Schröder, C. Seitz, S. Spannagel, A.D.R. Vargas Trevino, R. Walsh, C. Wissing

Deutsches Elektronen-Synchrotron, Hamburg, Germany

M. Aldaya Martin, V. Blobel, M. Centis Vignali, A.R. Draeger, J. Erfle, E. Garutti, K. Goebel, M. Görner, J. Haller, M. Hoffmann, R.S. Höing, H. Kirschenmann, R. Klanner, R. Kogler, J. Lange, T. Lapsien, T. Lenz, I. Marchesini, J. Ott, T. Peiffer, N. Pietsch, J. Poehlsen, T. Poehlsen, D. Rathjens, C. Sander, H. Schettler, P. Schleper, E. Schlieckau, A. Schmidt, M. Seidel, V. Sola, H. Stadie, G. Steinbrück, D. Troendle, E. Usai, L. Vanelderen, A. Vanhoefer

University of Hamburg, Hamburg, Germany

C. Barth, C. Baus, J. Berger, C. Böser, E. Butz, T. Chwalek, W. De Boer, A. Descroix, A. Dierlamm, M. Feindt, F. Frensch, M. Giffels, F. Hartmann [2], T. Hauth [2], U. Husemann, I. Katkov [5], A. Kornmayer [2], E. Kuznetsova, P. Lobelle Pardo, M.U. Mozer, Th. Müller, A. Nürnberg, G. Quast, K. Rabbertz, F. Ratnikov, S. Röcker, H.J. Simonis, F.M. Stober, R. Ulrich, J. Wagner-Kuhr, S. Wayand, T. Weiler, R. Wolf

Institut für Experimentelle Kernphysik, Karlsruhe, Germany

G. Anagnostou, G. Daskalakis, T. Geralis, V.A. Giakoumopoulou, A. Kyriakis, D. Loukas, A. Markou, C. Markou, A. Psallidas, I. Topsis-Giotis

Institute of Nuclear and Particle Physics (INPP), NCSR Demokritos, Aghia Paraskevi, Greece

S. Kesisoglou, A. Panagiotou, N. Saoulidou, E. Stiliaris

University of Athens, Athens, Greece

X. Aslanoglou, I. Evangelou, G. Flouris, C. Foudas, P. Kokkas, N. Manthos, I. Papadopoulos, E. Paradas

University of Ioánnina, Ioánnina, Greece

G. Bencze, C. Hajdu, P. Hidas, D. Horvath [16], F. Sikler, V. Veszpremi, G. Vesztergombi [17], A.J. Zsigmond

Wigner Research Centre for Physics, Budapest, Hungary

N. Beni, S. Czellar, J. Karancsi [18], J. Molnar, J. Palinkas, Z. Szillasi

Institute of Nuclear Research ATOMKI, Debrecen, Hungary

P. Raics, Z.L. Trocsanyi, B. Ujvari

University of Debrecen, Debrecen, Hungary

S.K. Swain

National Institute of Science Education and Research, Bhubaneswar, India

S.B. Beri, V. Bhatnagar, R. Gupta, U. Bhawandeep, A.K. Kalsi, M. Kaur, R. Kumar, M. Mittal, N. Nishu, J.B. Singh

Panjab University, Chandigarh, India

Ashok Kumar, Arun Kumar, S. Ahuja, A. Bhardwaj, B.C. Choudhary, A. Kumar, S. Malhotra, M. Naimuddin, K. Ranjan, V. Sharma

University of Delhi, Delhi, India

S. Banerjee, S. Bhattacharya, K. Chatterjee, S. Dutta, B. Gomber, Sa. Jain, Sh. Jain, R. Khurana, A. Modak, S. Mukherjee, D. Roy, S. Sarkar, M. Sharan

Saha Institute of Nuclear Physics, Kolkata, India

A. Abdulsalam, D. Dutta, S. Kailas, V. Kumar, A.K. Mohanty [2], L.M. Pant, P. Shukla, A. Topkar

Bhabha Atomic Research Centre, Mumbai, India

T. Aziz, S. Banerjee, S. Bhowmik [19], R.M. Chatterjee, R.K. Dewanjee, S. Dugad, S. Ganguly, S. Ghosh, M. Guchait, A. Gurtu [20], G. Kole, S. Kumar, M. Maity [19], G. Majumder, K. Mazumdar, G.B. Mohanty, B. Parida, K. Sudhakar, N. Wickramage [21]

Tata Institute of Fundamental Research, Mumbai, India

H. Bakhshiansohi, H. Behnamian, S.M. Etesami [22], A. Fahim [23], R. Goldouzian, M. Khakzad, M. Mohammadi Najafabadi, M. Naseri, S. Paktinat Mehdiabadi, F. Rezaei Hosseinabadi, B. Safarzadeh [24], M. Zeinali

Institute for Research in Fundamental Sciences (IPM), Tehran, Iran

M. Felcini, M. Grunewald

University College Dublin, Dublin, Ireland

M. Abbrescia [a,b], L. Barbone [a,b], C. Calabria [a,b], S.S. Chhibra [a,b], A. Colaleo [a], D. Creanza [a,c], N. De Filippis [a,c], M. De Palma [a,b], L. Fiore [a], G. Iaselli [a,c], G. Maggi [a,c], M. Maggi [a], S. My [a,c], S. Nuzzo [a,b], A. Pompili [a,b], G. Pugliese [a,c], R. Radogna [a,b,2], G. Selvaggi [a,b], L. Silvestris [a,2], G. Singh [a,b], R. Venditti [a,b], G. Zito [a]

[a] *INFN Sezione di Bari, Bari, Italy*
[b] *Università di Bari, Bari, Italy*
[c] *Politecnico di Bari, Bari, Italy*

G. Abbiendi [a], A.C. Benvenuti [a], D. Bonacorsi [a,b], S. Braibant-Giacomelli [a,b], L. Brigliadori [a,b], R. Campanini [a,b], P. Capiluppi [a,b], A. Castro [a,b], F.R. Cavallo [a], G. Codispoti [a,b], M. Cuffiani [a,b], G.M. Dallavalle [a], F. Fabbri [a], A. Fanfani [a,b], D. Fasanella [a,b], P. Giacomelli [a], C. Grandi [a], L. Guiducci [a,b], S. Marcellini [a], G. Masetti [a], A. Montanari [a], F.L. Navarria [a,b], A. Perrotta [a], F. Primavera [a,b], A.M. Rossi [a,b], T. Rovelli [a,b], G.P. Siroli [a,b], N. Tosi [a,b], R. Travaglini [a,b]

[a] *INFN Sezione di Bologna, Bologna, Italy*
[b] *Università di Bologna, Bologna, Italy*

S. Albergo [a,b], G. Cappello [a], M. Chiorboli [a,b], S. Costa [a,b], F. Giordano [a,2], R. Potenza [a,b], A. Tricomi [a,b], C. Tuve [a,b]

[a] *INFN Sezione di Catania, Catania, Italy*
[b] *Università di Catania, Catania, Italy*
[c] *CSFNSM, Catania, Italy*

G. Barbagli [a], V. Ciulli [a,b], C. Civinini [a], R. D'Alessandro [a,b], E. Focardi [a,b], E. Gallo [a], S. Gonzi [a,b], V. Gori [a,b,2], P. Lenzi [a,b], M. Meschini [a], S. Paoletti [a], G. Sguazzoni [a], A. Tropiano [a,b]

[a] *INFN Sezione di Firenze, Firenze, Italy*
[b] *Università di Firenze, Firenze, Italy*

L. Benussi, S. Bianco, F. Fabbri, D. Piccolo

INFN Laboratori Nazionali di Frascati, Frascati, Italy

R. Ferretti [a,b], F. Ferro [a], M. Lo Vetere [a,b], E. Robutti [a], S. Tosi [a,b]

[a] *INFN Sezione di Genova, Genova, Italy*
[b] *Università di Genova, Genova, Italy*

M.E. Dinardo [a,b], S. Fiorendi [a,b,2], S. Gennai [a,2], R. Gerosa [2], A. Ghezzi [a,b], P. Govoni [a,b], M.T. Lucchini [a,b,2], S. Malvezzi [a], R.A. Manzoni [a,b], A. Martelli [a,b], B. Marzocchi, D. Menasce [a], L. Moroni [a], M. Paganoni [a,b], D. Pedrini [a], S. Ragazzi [a,b], N. Redaelli [a], T. Tabarelli de Fatis [a,b]

[a] *INFN Sezione di Milano-Bicocca, Milano, Italy*
[b] *Università di Milano-Bicocca, Milano, Italy*

S. Buontempo [a], N. Cavallo [a,c], S. Di Guida [a,d,2], F. Fabozzi [a,c], A.O.M. Iorio [a,b], L. Lista [a], S. Meola [a,d,2], M. Merola [a], P. Paolucci [a,2]

[a] *INFN Sezione di Napoli, Napoli, Italy*
[b] *Università di Napoli 'Federico II', Napoli, Italy*
[c] *Università della Basilicata (Potenza), Napoli, Italy*
[d] *Università G. Marconi (Roma), Napoli, Italy*

P. Azzi [a], N. Bacchetta [a], M. Bellato [a], M. Biasotto [a,25], A. Branca [a,b], R. Carlin [a,b], P. Checchia [a], M. Dall'Osso [a,b], T. Dorigo [a], F. Fanzago [a], M. Galanti [a,b], F. Gasparini [a,b], U. Gasparini [a,b], P. Giubilato [a,b], A. Gozzelino [a], K. Kanishchev [a,c], S. Lacaprara [a], M. Margoni [a,b], A.T. Meneguzzo [a,b], J. Pazzini [a,b], N. Pozzobon [a,b], P. Ronchese [a,b], F. Simonetto [a,b], E. Torassa [a], M. Tosi [a,b], P. Zotto [a,b], A. Zucchetta [a,b]

[a] *INFN Sezione di Padova, Padova, Italy*
[b] *Università di Padova, Padova, Italy*
[c] *Università di Trento (Trento), Padova, Italy*

M. Gabusi [a,b], S.P. Ratti [a,b], V. Re [a], C. Riccardi [a,b], P. Salvini [a], P. Vitulo [a,b]

[a] *INFN Sezione di Pavia, Pavia, Italy*
[b] *Università di Pavia, Pavia, Italy*

M. Biasini [a,b], G.M. Bilei [a], D. Ciangottini [a,b], L. Fanò [a,b], P. Lariccia [a,b], G. Mantovani [a,b], M. Menichelli [a], F. Romeo [a,b], A. Saha [a], A. Santocchia [a,b], A. Spiezia [a,b,2]

[a] *INFN Sezione di Perugia, Perugia, Italy*
[b] *Università di Perugia, Perugia, Italy*

K. Androsov [a,26], P. Azzurri [a], G. Bagliesi [a], J. Bernardini [a], T. Boccali [a], G. Broccolo [a,c], R. Castaldi [a], M.A. Ciocci [a,26], R. Dell'Orso [a], S. Donato [a,c], F. Fiori [a,c], L. Foà [a,c], A. Giassi [a], M.T. Grippo [a,26], F. Ligabue [a,c], T. Lomtadze [a], L. Martini [a,b], A. Messineo [a,b], C.S. Moon [a,27], F. Palla [a,2], A. Rizzi [a,b], A. Savoy-Navarro [a,28], A.T. Serban [a], P. Spagnolo [a], P. Squillacioti [a,26], R. Tenchini [a], G. Tonelli [a,b], A. Venturi [a], P.G. Verdini [a], C. Vernieri [a,c,2]

[a] *INFN Sezione di Pisa, Pisa, Italy*
[b] *Università di Pisa, Pisa, Italy*
[c] *Scuola Normale Superiore di Pisa, Pisa, Italy*

L. Barone [a,b], F. Cavallari [a], G. D'imperio [a,b], D. Del Re [a,b], M. Diemoz [a], M. Grassi [a,b], C. Jorda [a], E. Longo [a,b], F. Margaroli [a,b], P. Meridiani [a], F. Micheli [a,b,2], S. Nourbakhsh [a,b], G. Organtini [a,b], R. Paramatti [a], S. Rahatlou [a,b], C. Rovelli [a], F. Santanastasio [a,b], L. Soffi [a,b,2], P. Traczyk [a,b]

[a] *INFN Sezione di Roma, Roma, Italy*
[b] *Università di Roma, Roma, Italy*

N. Amapane [a,b], R. Arcidiacono [a,c], S. Argiro [a,b,2], M. Arneodo [a,c], R. Bellan [a,b], C. Biino [a], N. Cartiglia [a], S. Casasso [a,b,2], M. Costa [a,b], A. Degano [a,b], N. Demaria [a], L. Finco [a,b], C. Mariotti [a], S. Maselli [a], E. Migliore [a,b], V. Monaco [a,b], M. Musich [a], M.M. Obertino [a,c,2], G. Ortona [a,b], L. Pacher [a,b], N. Pastrone [a], M. Pelliccioni [a], G.L. Pinna Angioni [a,b], A. Potenza [a,b], A. Romero [a,b], M. Ruspa [a,c], R. Sacchi [a,b], A. Solano [a,b], A. Staiano [a], U. Tamponi [a]

[a] *INFN Sezione di Torino, Torino, Italy*
[b] *Università di Torino, Torino, Italy*
[c] *Università del Piemonte Orientale (Novara), Torino, Italy*

S. Belforte [a], V. Candelise [a,b], M. Casarsa [a], F. Cossutti [a], G. Della Ricca [a,b], B. Gobbo [a], C. La Licata [a,b], M. Marone [a,b], A. Schizzi [a,b,2], T. Umer [a,b], A. Zanetti [a]

[a] *INFN Sezione di Trieste, Trieste, Italy*
[b] *Università di Trieste, Trieste, Italy*

S. Chang, A. Kropivnitskaya, S.K. Nam

Kangwon National University, Chunchon, Republic of Korea

D.H. Kim, G.N. Kim, M.S. Kim, D.J. Kong, S. Lee, Y.D. Oh, H. Park, A. Sakharov, D.C. Son

Kyungpook National University, Daegu, Republic of Korea

T.J. Kim

Chonbuk National University, Jeonju, Republic of Korea

J.Y. Kim, S. Song

Chonnam National University, Institute for Universe and Elementary Particles, Kwangju, Republic of Korea

S. Choi, D. Gyun, B. Hong, M. Jo, H. Kim, Y. Kim, B. Lee, K.S. Lee, S.K. Park, Y. Roh

Korea University, Seoul, Republic of Korea

M. Choi, J.H. Kim, I.C. Park, G. Ryu, M.S. Ryu

University of Seoul, Seoul, Republic of Korea

Y. Choi, Y.K. Choi, J. Goh, D. Kim, E. Kwon, J. Lee, H. Seo, I. Yu

Sungkyunkwan University, Suwon, Republic of Korea

A. Juodagalvis

Vilnius University, Vilnius, Lithuania

J.R. Komaragiri, M.A.B. Md Ali

National Centre for Particle Physics, Universiti Malaya, Kuala Lumpur, Malaysia

H. Castilla-Valdez, E. De La Cruz-Burelo, I. Heredia-de La Cruz [29], A. Hernandez-Almada, R. Lopez-Fernandez, A. Sanchez-Hernandez

Centro de Investigacion y de Estudios Avanzados del IPN, Mexico City, Mexico

S. Carrillo Moreno, F. Vazquez Valencia

Universidad Iberoamericana, Mexico City, Mexico

I. Pedraza, H.A. Salazar Ibarguen

Benemerita Universidad Autonoma de Puebla, Puebla, Mexico

E. Casimiro Linares, A. Morelos Pineda

Universidad Autónoma de San Luis Potosí, San Luis Potosí, Mexico

D. Krofcheck

University of Auckland, Auckland, New Zealand

P.H. Butler, S. Reucroft

University of Canterbury, Christchurch, New Zealand

A. Ahmad, M. Ahmad, Q. Hassan, H.R. Hoorani, S. Khalid, W.A. Khan, T. Khurshid, M.A. Shah, M. Shoaib

National Centre for Physics, Quaid-I-Azam University, Islamabad, Pakistan

H. Bialkowska, M. Bluj, B. Boimska, T. Frueboes, M. Górski, M. Kazana, K. Nawrocki,
K. Romanowska-Rybinska, M. Szleper, P. Zalewski

National Centre for Nuclear Research, Swierk, Poland

G. Brona, K. Bunkowski, M. Cwiok, W. Dominik, K. Doroba, A. Kalinowski, M. Konecki, J. Krolikowski,
M. Misiura, M. Olszewski, W. Wolszczak

Institute of Experimental Physics, Faculty of Physics, University of Warsaw, Warsaw, Poland

P. Bargassa, C. Beirão Da Cruz E Silva, P. Faccioli, P.G. Ferreira Parracho, M. Gallinaro, L. Lloret Iglesias,
F. Nguyen, J. Rodrigues Antunes, J. Seixas, J. Varela, P. Vischia

Laboratório de Instrumentação e Física Experimental de Partículas, Lisboa, Portugal

S. Afanasiev, P. Bunin, M. Gavrilenko, I. Golutvin, I. Gorbunov, A. Kamenev, V. Karjavin, V. Konoplyanikov,
A. Lanev, A. Malakhov, V. Matveev [30], P. Moisenz, V. Palichik, V. Perelygin, S. Shmatov, N. Skatchkov,
V. Smirnov, A. Zarubin

Joint Institute for Nuclear Research, Dubna, Russia

V. Golovtsov, Y. Ivanov, V. Kim [31], P. Levchenko, V. Murzin, V. Oreshkin, I. Smirnov, V. Sulimov, L. Uvarov,
S. Vavilov, A. Vorobyev, An. Vorobyev

Petersburg Nuclear Physics Institute, Gatchina (St. Petersburg), Russia

Yu. Andreev, A. Dermenev, S. Gninenko, N. Golubev, M. Kirsanov, N. Krasnikov, A. Pashenkov, D. Tlisov,
A. Toropin

Institute for Nuclear Research, Moscow, Russia

V. Epshteyn, V. Gavrilov, N. Lychkovskaya, V. Popov, G. Safronov, S. Semenov, A. Spiridonov, V. Stolin,
E. Vlasov, A. Zhokin

Institute for Theoretical and Experimental Physics, Moscow, Russia

V. Andreev, M. Azarkin, I. Dremin, M. Kirakosyan, A. Leonidov, G. Mesyats, S.V. Rusakov, A. Vinogradov

P.N. Lebedev Physical Institute, Moscow, Russia

A. Belyaev, E. Boos, A. Ershov, A. Gribushin, V. Klyukhin, O. Kodolova, V. Korotkikh, I. Lokhtin,
S. Obraztsov, S. Petrushanko, V. Savrin, A. Snigirev, I. Vardanyan

Skobeltsyn Institute of Nuclear Physics, Lomonosov Moscow State University, Moscow, Russia

I. Azhgirey, I. Bayshev, S. Bitioukov, V. Kachanov, A. Kalinin, D. Konstantinov, V. Krychkine, V. Petrov,
R. Ryutin, A. Sobol, L. Tourtchanovitch, S. Troshin, N. Tyurin, A. Uzunian, A. Volkov

State Research Center of Russian Federation, Institute for High Energy Physics, Protvino, Russia

P. Adzic [32], M. Ekmedzic, J. Milosevic, V. Rekovic

University of Belgrade, Faculty of Physics and Vinca Institute of Nuclear Sciences, Belgrade, Serbia

J. Alcaraz Maestre, C. Battilana, E. Calvo, M. Cerrada, M. Chamizo Llatas, N. Colino, B. De La Cruz, A. Delgado Peris, D. Domínguez Vázquez, A. Escalante Del Valle, C. Fernandez Bedoya, J.P. Fernández Ramos, J. Flix, M.C. Fouz, P. Garcia-Abia, O. Gonzalez Lopez, S. Goy Lopez, J.M. Hernandez, M.I. Josa, E. Navarro De Martino, A. Pérez-Calero Yzquierdo, J. Puerta Pelayo, A. Quintario Olmeda, I. Redondo, L. Romero, M.S. Soares

Centro de Investigaciones Energéticas Medioambientales y Tecnológicas (CIEMAT), Madrid, Spain

C. Albajar, J.F. de Trocóniz, M. Missiroli, D. Moran

Universidad Autónoma de Madrid, Madrid, Spain

H. Brun, J. Cuevas, J. Fernandez Menendez, S. Folgueras, I. Gonzalez Caballero

Universidad de Oviedo, Oviedo, Spain

J.A. Brochero Cifuentes, I.J. Cabrillo, A. Calderon, J. Duarte Campderros, M. Fernandez, G. Gomez, A. Graziano, A. Lopez Virto, J. Marco, R. Marco, C. Martinez Rivero, F. Matorras, F.J. Munoz Sanchez, J. Piedra Gomez, T. Rodrigo, A.Y. Rodríguez-Marrero, A. Ruiz-Jimeno, L. Scodellaro, I. Vila, R. Vilar Cortabitarte

Instituto de Física de Cantabria (IFCA), CSIC-Universidad de Cantabria, Santander, Spain

D. Abbaneo, E. Auffray, G. Auzinger, M. Bachtis, P. Baillon, A.H. Ball, D. Barney, A. Benaglia, J. Bendavid, L. Benhabib, J.F. Benitez, C. Bernet [7], G. Bianchi, P. Bloch, A. Bocci, A. Bonato, O. Bondu, C. Botta, H. Breuker, T. Camporesi, G. Cerminara, S. Colafranceschi [33], M. D'Alfonso, D. d'Enterria, A. Dabrowski, A. David, F. De Guio, A. De Roeck, S. De Visscher, E. Di Marco, M. Dobson, M. Dordevic, N. Dupont-Sagorin, A. Elliott-Peisert, J. Eugster, G. Franzoni, W. Funk, D. Gigi, K. Gill, D. Giordano, M. Girone, F. Glege, R. Guida, S. Gundacker, M. Guthoff, J. Hammer, M. Hansen, P. Harris, J. Hegeman, V. Innocente, P. Janot, K. Kousouris, K. Krajczar, P. Lecoq, C. Lourenço, N. Magini, L. Malgeri, M. Mannelli, J. Marrouche, L. Masetti, F. Meijers, S. Mersi, E. Meschi, F. Moortgat, S. Morovic, M. Mulders, P. Musella, L. Orsini, L. Pape, E. Perez, L. Perrozzi, A. Petrilli, G. Petrucciani, A. Pfeiffer, M. Pierini, M. Pimiä, D. Piparo, M. Plagge, A. Racz, G. Rolandi [34], M. Rovere, H. Sakulin, C. Schäfer, C. Schwick, A. Sharma, P. Siegrist, P. Silva, M. Simon, P. Sphicas [35], D. Spiga, J. Steggemann, B. Stieger, M. Stoye, Y. Takahashi, D. Treille, A. Tsirou, G.I. Veres [17], J.R. Vlimant, N. Wardle, H.K. Wöhri, H. Wollny, W.D. Zeuner

CERN, European Organization for Nuclear Research, Geneva, Switzerland

W. Bertl, K. Deiters, W. Erdmann, R. Horisberger, Q. Ingram, H.C. Kaestli, D. Kotlinski, U. Langenegger, D. Renker, T. Rohe

Paul Scherrer Institut, Villigen, Switzerland

F. Bachmair, L. Bäni, L. Bianchini, M.A. Buchmann, B. Casal, N. Chanon, G. Dissertori, M. Dittmar, M. Donegà, M. Dünser, P. Eller, C. Grab, D. Hits, J. Hoss, W. Lustermann, B. Mangano, A.C. Marini, P. Martinez Ruiz del Arbol, M. Masciovecchio, D. Meister, N. Mohr, C. Nägeli [36], F. Nessi-Tedaldi, F. Pandolfi, F. Pauss, M. Peruzzi, M. Quittnat, L. Rebane, M. Rossini, A. Starodumov [37], M. Takahashi, K. Theofilatos, R. Wallny, H.A. Weber

Institute for Particle Physics, ETH Zurich, Zurich, Switzerland

C. Amsler [38], M.F. Canelli, V. Chiochia, A. De Cosa, A. Hinzmann, T. Hreus, B. Kilminster, C. Lange, B. Millan Mejias, J. Ngadiuba, P. Robmann, F.J. Ronga, S. Taroni, M. Verzetti, Y. Yang

Universität Zürich, Zurich, Switzerland

M. Cardaci, K.H. Chen, C. Ferro, C.M. Kuo, W. Lin, Y.J. Lu, R. Volpe, S.S. Yu

National Central University, Chung-Li, Taiwan

P. Chang, Y.H. Chang, Y.W. Chang, Y. Chao, K.F. Chen, P.H. Chen, C. Dietz, U. Grundler, W.-S. Hou, K.Y. Kao, Y.J. Lei, Y.F. Liu, R.-S. Lu, D. Majumder, E. Petrakou, Y.M. Tzeng, R. Wilken

National Taiwan University (NTU), Taipei, Taiwan

B. Asavapibhop, N. Srimanobhas, N. Suwonjandee

Chulalongkorn University, Faculty of Science, Department of Physics, Bangkok, Thailand

A. Adiguzel, M.N. Bakirci [39], S. Cerci [40], C. Dozen, I. Dumanoglu, E. Eskut, S. Girgis, G. Gokbulut, E. Gurpinar, I. Hos, E.E. Kangal, A. Kayis Topaksu, G. Onengut [41], K. Ozdemir, S. Ozturk [39], A. Polatoz, D. Sunar Cerci [40], B. Tali [40], H. Topakli [39], M. Vergili

Cukurova University, Adana, Turkey

I.V. Akin, B. Bilin, S. Bilmis, H. Gamsizkan [42], G. Karapinar [43], K. Ocalan [44], S. Sekmen, U.E. Surat, M. Yalvac, M. Zeyrek

Middle East Technical University, Physics Department, Ankara, Turkey

E. Gülmez, B. Isildak [45], M. Kaya [46], O. Kaya [47]

Bogazici University, Istanbul, Turkey

K. Cankocak, F.I. Vardarlı

Istanbul Technical University, Istanbul, Turkey

L. Levchuk, P. Sorokin

National Scientific Center, Kharkov Institute of Physics and Technology, Kharkov, Ukraine

J.J. Brooke, E. Clement, D. Cussans, H. Flacher, R. Frazier, J. Goldstein, M. Grimes, G.P. Heath, H.F. Heath, J. Jacob, L. Kreczko, C. Lucas, Z. Meng, D.M. Newbold [48], S. Paramesvaran, A. Poll, S. Senkin, V.J. Smith, T. Williams

University of Bristol, Bristol, United Kingdom

A. Belyaev [49], C. Brew, R.M. Brown, D.J.A. Cockerill, J.A. Coughlan, K. Harder, S. Harper, E. Olaiya, D. Petyt, C.H. Shepherd-Themistocleous, A. Thea, I.R. Tomalin, W.J. Womersley, S.D. Worm

Rutherford Appleton Laboratory, Didcot, United Kingdom

M. Baber, R. Bainbridge, O. Buchmuller, D. Burton, D. Colling, N. Cripps, M. Cutajar, P. Dauncey, G. Davies, M. Della Negra, P. Dunne, W. Ferguson, J. Fulcher, D. Futyan, A. Gilbert, G. Hall, G. Iles, M. Jarvis, G. Karapostoli, M. Kenzie, R. Lane, R. Lucas [48], L. Lyons, A.-M. Magnan, S. Malik, B. Mathias, J. Nash, A. Nikitenko [37], J. Pela, M. Pesaresi, K. Petridis, D.M. Raymond, S. Rogerson, A. Rose, C. Seez, P. Sharp [†], A. Tapper, M. Vazquez Acosta, T. Virdee, S.C. Zenz

Imperial College, London, United Kingdom

J.E. Cole, P.R. Hobson, A. Khan, P. Kyberd, D. Leggat, D. Leslie, W. Martin, I.D. Reid, P. Symonds, L. Teodorescu, M. Turner

Brunel University, Uxbridge, United Kingdom

J. Dittmann, K. Hatakeyama, A. Kasmi, H. Liu, T. Scarborough

Baylor University, Waco, USA

O. Charaf, S.I. Cooper, C. Henderson, P. Rumerio

The University of Alabama, Tuscaloosa, USA

A. Avetisyan, T. Bose, C. Fantasia, P. Lawson, C. Richardson, J. Rohlf, J. St. John, L. Sulak

Boston University, Boston, USA

J. Alimena, E. Berry, S. Bhattacharya, G. Christopher, D. Cutts, Z. Demiragli, N. Dhingra, A. Ferapontov,
A. Garabedian, U. Heintz, G. Kukartsev, E. Laird, G. Landsberg, M. Luk, M. Narain, M. Segala,
T. Sinthuprasith, T. Speer, J. Swanson

Brown University, Providence, USA

R. Breedon, G. Breto, M. Calderon De La Barca Sanchez, S. Chauhan, M. Chertok, J. Conway, R. Conway,
P.T. Cox, R. Erbacher, M. Gardner, W. Ko, R. Lander, T. Miceli, M. Mulhearn, D. Pellett, J. Pilot,
F. Ricci-Tam, M. Searle, S. Shalhout, J. Smith, M. Squires, D. Stolp, M. Tripathi, S. Wilbur, R. Yohay

University of California, Davis, Davis, USA

R. Cousins, P. Everaerts, C. Farrell, J. Hauser, M. Ignatenko, G. Rakness, E. Takasugi, V. Valuev, M. Weber

University of California, Los Angeles, USA

K. Burt, R. Clare, J. Ellison, J.W. Gary, G. Hanson, J. Heilman, M. Ivova Rikova, P. Jandir, E. Kennedy,
F. Lacroix, O.R. Long, A. Luthra, M. Malberti, H. Nguyen, M. Olmedo Negrete, A. Shrinivas,
S. Sumowidagdo, S. Wimpenny

University of California, Riverside, Riverside, USA

W. Andrews, J.G. Branson, G.B. Cerati, S. Cittolin, R.T. D'Agnolo, D. Evans, A. Holzner, R. Kelley, D. Klein,
M. Lebourgeois, J. Letts, I. Macneill, D. Olivito, S. Padhi, C. Palmer, M. Pieri, M. Sani, V. Sharma, S. Simon,
E. Sudano, M. Tadel, Y. Tu, A. Vartak, C. Welke, F. Würthwein, A. Yagil

University of California, San Diego, La Jolla, USA

D. Barge, J. Bradmiller-Feld, C. Campagnari, T. Danielson, A. Dishaw, K. Flowers, M. Franco Sevilla,
P. Geffert, C. George, F. Golf, L. Gouskos, J. Incandela, C. Justus, N. Mccoll, J. Richman, D. Stuart, W. To,
C. West, J. Yoo

University of California, Santa Barbara, Santa Barbara, USA

A. Apresyan, A. Bornheim, J. Bunn, Y. Chen, J. Duarte, A. Mott, H.B. Newman, C. Pena, C. Rogan,
M. Spiropulu, V. Timciuc, R. Wilkinson, S. Xie, R.Y. Zhu

California Institute of Technology, Pasadena, USA

V. Azzolini, A. Calamba, B. Carlson, T. Ferguson, Y. Iiyama, M. Paulini, J. Russ, H. Vogel, I. Vorobiev

Carnegie Mellon University, Pittsburgh, USA

J.P. Cumalat, W.T. Ford, A. Gaz, E. Luiggi Lopez, U. Nauenberg, J.G. Smith, K. Stenson, K.A. Ulmer,
S.R. Wagner

University of Colorado at Boulder, Boulder, USA

J. Alexander, A. Chatterjee, J. Chu, S. Dittmer, N. Eggert, N. Mirman, G. Nicolas Kaufman, J.R. Patterson,
A. Ryd, E. Salvati, L. Skinnari, W. Sun, W.D. Teo, J. Thom, J. Thompson, J. Tucker, Y. Weng, L. Winstrom,
P. Wittich

Cornell University, Ithaca, USA

D. Winn

Fairfield University, Fairfield, USA

S. Abdullin, M. Albrow, J. Anderson, G. Apollinari, L.A.T. Bauerdick, A. Beretvas, J. Berryhill, P.C. Bhat, G. Bolla, K. Burkett, J.N. Butler, H.W.K. Cheung, F. Chlebana, S. Cihangir, V.D. Elvira, I. Fisk, J. Freeman, Y. Gao, E. Gottschalk, L. Gray, D. Green, S. Grünendahl, O. Gutsche, J. Hanlon, D. Hare, R.M. Harris, J. Hirschauer, B. Hooberman, S. Jindariani, M. Johnson, U. Joshi, K. Kaadze, B. Klima, B. Kreis, S. Kwan, J. Linacre, D. Lincoln, R. Lipton, T. Liu, J. Lykken, K. Maeshima, J.M. Marraffino, V.I. Martinez Outschoorn, S. Maruyama, D. Mason, P. McBride, P. Merkel, K. Mishra, S. Mrenna, Y. Musienko [30], S. Nahn, C. Newman-Holmes, V. O'Dell, O. Prokofyev, E. Sexton-Kennedy, S. Sharma, A. Soha, W.J. Spalding, L. Spiegel, L. Taylor, S. Tkaczyk, N.V. Tran, L. Uplegger, E.W. Vaandering, R. Vidal, A. Whitbeck, J. Whitmore, F. Yang

Fermi National Accelerator Laboratory, Batavia, USA

D. Acosta, P. Avery, P. Bortignon, D. Bourilkov, M. Carver, T. Cheng, D. Curry, S. Das, M. De Gruttola, G.P. Di Giovanni, R.D. Field, M. Fisher, I.K. Furic, J. Hugon, J. Konigsberg, A. Korytov, T. Kypreos, J.F. Low, K. Matchev, P. Milenovic [50], G. Mitselmakher, L. Muniz, A. Rinkevicius, L. Shchutska, M. Snowball, D. Sperka, J. Yelton, M. Zakaria

University of Florida, Gainesville, USA

S. Hewamanage, S. Linn, P. Markowitz, G. Martinez, J.L. Rodriguez

Florida International University, Miami, USA

T. Adams, A. Askew, J. Bochenek, B. Diamond, J. Haas, S. Hagopian, V. Hagopian, K.F. Johnson, H. Prosper, V. Veeraraghavan, M. Weinberg

Florida State University, Tallahassee, USA

M.M. Baarmand, M. Hohlmann, H. Kalakhety, F. Yumiceva

Florida Institute of Technology, Melbourne, USA

M.R. Adams, L. Apanasevich, V.E. Bazterra, D. Berry, R.R. Betts, I. Bucinskaite, R. Cavanaugh, O. Evdokimov, L. Gauthier, C.E. Gerber, D.J. Hofman, S. Khalatyan, P. Kurt, D.H. Moon, C. O'Brien, C. Silkworth, P. Turner, N. Varelas

University of Illinois at Chicago (UIC), Chicago, USA

E.A. Albayrak [51], B. Bilki [52], W. Clarida, K. Dilsiz, F. Duru, M. Haytmyradov, J.-P. Merlo, H. Mermerkaya [53], A. Mestvirishvili, A. Moeller, J. Nachtman, H. Ogul, Y. Onel, F. Ozok [51], A. Penzo, R. Rahmat, S. Sen, P. Tan, E. Tiras, J. Wetzel, T. Yetkin [54], K. Yi

The University of Iowa, Iowa City, USA

B.A. Barnett, B. Blumenfeld, S. Bolognesi, D. Fehling, A.V. Gritsan, P. Maksimovic, C. Martin, M. Swartz

Johns Hopkins University, Baltimore, USA

P. Baringer, A. Bean, G. Benelli, C. Bruner, R.P. Kenny III, M. Malek, M. Murray, D. Noonan, S. Sanders, J. Sekaric, R. Stringer, Q. Wang, J.S. Wood

The University of Kansas, Lawrence, USA

A.F. Barfuss, I. Chakaberia, A. Ivanov, S. Khalil, M. Makouski, Y. Maravin, L.K. Saini, S. Shrestha, N. Skhirtladze, I. Svintradze

Kansas State University, Manhattan, USA

J. Gronberg, D. Lange, F. Rebassoo, D. Wright

Lawrence Livermore National Laboratory, Livermore, USA

A. Baden, A. Belloni, B. Calvert, S.C. Eno, J.A. Gomez, N.J. Hadley, R.G. Kellogg, T. Kolberg, Y. Lu, M. Marionneau, A.C. Mignerey, K. Pedro, A. Skuja, M.B. Tonjes, S.C. Tonwar

University of Maryland, College Park, USA

A. Apyan, R. Barbieri, G. Bauer, W. Busza, I.A. Cali, M. Chan, L. Di Matteo, V. Dutta, G. Gomez Ceballos, M. Goncharov, D. Gulhan, M. Klute, Y.S. Lai, Y.-J. Lee, A. Levin, P.D. Luckey, T. Ma, C. Paus, D. Ralph, C. Roland, G. Roland, G.S.F. Stephans, F. Stöckli, K. Sumorok, D. Velicanu, J. Veverka, B. Wyslouch, M. Yang, M. Zanetti, V. Zhukova

Massachusetts Institute of Technology, Cambridge, USA

B. Dahmes, A. Gude, S.C. Kao, K. Klapoetke, Y. Kubota, J. Mans, N. Pastika, R. Rusack, A. Singovsky, N. Tambe, J. Turkewitz

University of Minnesota, Minneapolis, USA

J.G. Acosta, S. Oliveros

University of Mississippi, Oxford, USA

E. Avdeeva, K. Bloom, S. Bose, D.R. Claes, A. Dominguez, R. Gonzalez Suarez, J. Keller, D. Knowlton, I. Kravchenko, J. Lazo-Flores, S. Malik, F. Meier, G.R. Snow, M. Zvada

University of Nebraska-Lincoln, Lincoln, USA

J. Dolen, A. Godshalk, I. Iashvili, A. Kharchilava, A. Kumar, S. Rappoccio

State University of New York at Buffalo, Buffalo, USA

G. Alverson, E. Barberis, D. Baumgartel, M. Chasco, J. Haley, A. Massironi, D.M. Morse, D. Nash, T. Orimoto, D. Trocino, R.-J. Wang, D. Wood, J. Zhang

Northeastern University, Boston, USA

K.A. Hahn, A. Kubik, N. Mucia, N. Odell, B. Pollack, A. Pozdnyakov, M. Schmitt, S. Stoynev, K. Sung, M. Velasco, S. Won

Northwestern University, Evanston, USA

A. Brinkerhoff, K.M. Chan, A. Drozdetskiy, M. Hildreth, C. Jessop, D.J. Karmgard, N. Kellams, K. Lannon, W. Luo, S. Lynch, N. Marinelli, T. Pearson, M. Planer, R. Ruchti, N. Valls, M. Wayne, M. Wolf, A. Woodard

University of Notre Dame, Notre Dame, USA

L. Antonelli, J. Brinson, B. Bylsma, L.S. Durkin, S. Flowers, C. Hill, R. Hughes, K. Kotov, T.Y. Ling, D. Puigh, M. Rodenburg, G. Smith, B.L. Winer, H. Wolfe, H.W. Wulsin

The Ohio State University, Columbus, USA

O. Driga, P. Elmer, P. Hebda, A. Hunt, S.A. Koay, P. Lujan, D. Marlow, T. Medvedeva, M. Mooney, J. Olsen, P. Piroué, X. Quan, H. Saka, D. Stickland [2], C. Tully, J.S. Werner, A. Zuranski

Princeton University, Princeton, USA

E. Brownson, H. Mendez, J.E. Ramirez Vargas

University of Puerto Rico, Mayaguez, USA

V.E. Barnes, D. Benedetti, D. Bortoletto, M. De Mattia, L. Gutay, Z. Hu, M.K. Jha, M. Jones, K. Jung, M. Kress, N. Leonardo, D. Lopes Pegna, V. Maroussov, D.H. Miller, N. Neumeister, B.C. Radburn-Smith, X. Shi, I. Shipsey, D. Silvers, A. Svyatkovskiy, F. Wang, W. Xie, L. Xu, H.D. Yoo, J. Zablocki, Y. Zheng

Purdue University, West Lafayette, USA

N. Parashar, J. Stupak

Purdue University Calumet, Hammond, USA

A. Adair, B. Akgun, K.M. Ecklund, F.J.M. Geurts, W. Li, B. Michlin, B.P. Padley, R. Redjimi, J. Roberts, J. Zabel

Rice University, Houston, USA

B. Betchart, A. Bodek, R. Covarelli, P. de Barbaro, R. Demina, Y. Eshaq, T. Ferbel, A. Garcia-Bellido, P. Goldenzweig, J. Han, A. Harel, A. Khukhunaishvili, G. Petrillo, D. Vishnevskiy

University of Rochester, Rochester, USA

R. Ciesielski, L. Demortier, K. Goulianos, G. Lungu, C. Mesropian

The Rockefeller University, New York, USA

S. Arora, A. Barker, J.P. Chou, C. Contreras-Campana, E. Contreras-Campana, D. Duggan, D. Ferencek, Y. Gershtein, R. Gray, E. Halkiadakis, D. Hidas, S. Kaplan, A. Lath, S. Panwalkar, M. Park, R. Patel, S. Salur, S. Schnetzer, S. Somalwar, R. Stone, S. Thomas, P. Thomassen, M. Walker

Rutgers, The State University of New Jersey, Piscataway, USA

K. Rose, S. Spanier, A. York

University of Tennessee, Knoxville, USA

O. Bouhali [55], A. Castaneda Hernandez, R. Eusebi, W. Flanagan, J. Gilmore, T. Kamon [56], V. Khotilovich, V. Krutelyov, R. Montalvo, I. Osipenkov, Y. Pakhotin, A. Perloff, J. Roe, A. Rose, A. Safonov, T. Sakuma, I. Suarez, A. Tatarinov

Texas A&M University, College Station, USA

N. Akchurin, C. Cowden, J. Damgov, C. Dragoiu, P.R. Dudero, J. Faulkner, K. Kovitanggoon, S. Kunori, S.W. Lee, T. Libeiro, I. Volobouev

Texas Tech University, Lubbock, USA

E. Appelt, A.G. Delannoy, S. Greene, A. Gurrola, W. Johns, C. Maguire, Y. Mao, A. Melo, M. Sharma, P. Sheldon, B. Snook, S. Tuo, J. Velkovska

Vanderbilt University, Nashville, USA

M.W. Arenton, S. Boutle, B. Cox, B. Francis, J. Goodell, R. Hirosky, A. Ledovskoy, H. Li, C. Lin, C. Neu, J. Wood

University of Virginia, Charlottesville, USA

C. Clarke, R. Harr, P.E. Karchin, C. Kottachchi Kankanamge Don, P. Lamichhane, J. Sturdy

Wayne State University, Detroit, USA

D.A. Belknap, D. Carlsmith, M. Cepeda, S. Dasu, L. Dodd, S. Duric, E. Friis, R. Hall-Wilton, M. Herndon, A. Hervé, P. Klabbers, A. Lanaro, C. Lazaridis, A. Levine, R. Loveless, A. Mohapatra, I. Ojalvo, T. Perry, G.A. Pierro, G. Polese, I. Ross, T. Sarangi, A. Savin, W.H. Smith, D. Taylor, P. Verwilligen, C. Vuosalo, N. Woods

University of Wisconsin, Madison, USA

[4] Also at National Institute of Chemical Physics and Biophysics, Tallinn, Estonia.

[5] Also at Skobeltsyn Institute of Nuclear Physics, Lomonosov Moscow State University, Moscow, Russia.

[6] Also at Universidade Estadual de Campinas, Campinas, Brazil.

[7] Also at Laboratoire Leprince-Ringuet, Ecole Polytechnique, IN2P3-CNRS, Palaiseau, France.

[8] Also at Joint Institute for Nuclear Research, Dubna, Russia.

[9] Also at Suez University, Suez, Egypt.

[10] Also at Cairo University, Cairo, Egypt.

[11] Also at Fayoum University, El-Fayoum, Egypt.

[12] Also at British University in Egypt, Cairo, Egypt.

[13] Now at Ain Shams University, Cairo, Egypt.

[14] Also at Université de Haute Alsace, Mulhouse, France.

[15] Also at Brandenburg University of Technology, Cottbus, Germany.

[16] Also at Institute of Nuclear Research ATOMKI, Debrecen, Hungary.

[17] Also at Eötvös Loránd University, Budapest, Hungary.

[18] Also at University of Debrecen, Debrecen, Hungary.

[19] Also at University of Visva-Bharati, Santiniketan, India.

[20] Now at King Abdulaziz University, Jeddah, Saudi Arabia.

[21] Also at University of Ruhuna, Matara, Sri Lanka.

[22] Also at Isfahan University of Technology, Isfahan, Iran.

[23] Also at Sharif University of Technology, Tehran, Iran.

[24] Also at Plasma Physics Research Center, Science and Research Branch, Islamic Azad University, Tehran, Iran.

[25] Also at Laboratori Nazionali di Legnaro dell'INFN, Legnaro, Italy.

[26] Also at Università degli Studi di Siena, Siena, Italy.

[27] Also at Centre National de la Recherche Scientifique (CNRS) – IN2P3, Paris, France.

[28] Also at Purdue University, West Lafayette, USA.

[29] Also at Universidad Michoacana de San Nicolas de Hidalgo, Morelia, Mexico.

[30] Also at Institute for Nuclear Research, Moscow, Russia.

[31] Also at St. Petersburg State Polytechnical University, St. Petersburg, Russia.

[32] Also at Faculty of Physics, University of Belgrade, Belgrade, Serbia.

[33] Also at Facoltà Ingegneria, Università di Roma, Roma, Italy.

[34] Also at Scuola Normale e Sezione dell'INFN, Pisa, Italy.

[35] Also at University of Athens, Athens, Greece.

[36] Also at Paul Scherrer Institut, Villigen, Switzerland.

[37] Also at Institute for Theoretical and Experimental Physics, Moscow, Russia.

[38] Also at Albert Einstein Center for Fundamental Physics, Bern, Switzerland.

[39] Also at Gaziosmanpasa University, Tokat, Turkey.

[40] Also at Adiyaman University, Adiyaman, Turkey.

[41] Also at Cag University, Mersin, Turkey.

[42] Also at Anadolu University, Eskisehir, Turkey.

[43] Also at Izmir Institute of Technology, Izmir, Turkey.

[44] Also at Necmettin Erbakan University, Konya, Turkey.

[45] Also at Ozyegin University, Istanbul, Turkey.

[46] Also at Marmara University, Istanbul, Turkey.

[47] Also at Kafkas University, Kars, Turkey.

[48] Also at Rutherford Appleton Laboratory, Didcot, United Kingdom.

[49] Also at School of Physics and Astronomy, University of Southampton, Southampton, United Kingdom.

[50] Also at University of Belgrade, Faculty of Physics and Vinca Institute of Nuclear Sciences, Belgrade, Serbia.

[51] Also at Mimar Sinan University, Istanbul, Istanbul, Turkey.

[52] Also at Argonne National Laboratory, Argonne, USA.

[53] Also at Erzincan University, Erzincan, Turkey.

[54] Also at Yildiz Technical University, Istanbul, Turkey.

[55] Also at Texas A&M University at Qatar, Doha, Qatar.

[56] Also at Kyungpook National University, Daegu, Republic of Korea.